Published in final edited form as:

Cell Microbiol. 2018 January ; 20(1): . doi:10.1111/cmi.12787.

N-(3-oxo-acyl)-homoserine lactone induces apoptosis primarily through a mitochondrial pathway in fibroblasts

Aaron M. Neely[1,#], **Guoping Zhao**[1,4], **Christian Schwarzer**[3], **Nicole S. Stivers**[1], **Aaron G. Whitt**[1], **Shuhan Meng**[1], **Joseph A. Burlison**[2], **Terry E. Machen**[3], and **Chi Li**[1,*]

[1]Molecular Targets Program, University of Louisville, Louisville, KY 40202

[2]Structural Biology Program, James Graham Brown Cancer Center, Departments of Medicine, Pharmacology and Toxicology, University of Louisville, Louisville, KY 40202

[3]Department of Molecular and Cell Biology, University of California, Berkeley, CA 94720

[4]Institute of Technical Biology and Agriculture Engineering, Hefei Institutes of Physical Science, Chinese Academy of Sciences, Hefei, Anhui Province, P.R. China 230031

Abstract

N-(3-oxododecanoyl)-homoserine lactone (C12) is produced by *Pseudomonas aeruginosa* to function as a quorum-sensing molecule for bacteria-bacteria communication. C12 is also known to influence many aspects of human host cell physiology, including induction of cell death. However, the signaling pathway(s) leading to C12-triggered cell death is (are) still not completely known. To clarify cell death signaling induced by C12, we examined mouse embryonic fibroblasts (MEFs) deficient in “initiator” caspases or “effector” caspases. Our data indicate that C12 selectively induces the mitochondria-dependent intrinsic apoptotic pathway by quickly triggering mitochondrial outer membrane permeabilization (MOMP). Importantly, the activities of C12 to permeabilize mitochondria is independent of activation of both “initiator” and “effector” caspases. Furthermore, C12 directly induces MOMP *in vitro*. Overall, our study suggests a mitochondrial apoptotic signaling pathway triggered by C12, in which C12 or its metabolite(s) acts on mitochondria to permeabilize mitochondria, leading to activation of apoptosis.

Keywords

homoserine lactone; apoptosis; caspase; mitochondria

[*]To whom correspondence should be addressed: Chi Li, Clinical and Translational Research Building, Room 418, 505 South Hancock St., Louisville, KY 40202, Tel: 502-852-0600, Fax: 502-852-3661, chi.li@louisville.edu.
[#]Current address: Department of Cancer Biology, City of Hope National Medical Center, Duarte, CA 91010

AUTHOR CONTRIBUTION

TM and CL designed research. AMN, GZ, CS, NSS, AGW, SM and JAB performed research. AMN, GZ, CS, NSS, AGW, SM, JAB, TM, and CL analyzed data. AMN and CL wrote the paper.

DECLARATIONS OF INTERESTS

There is no actual, potential, or perceived conflict of interest to disclose.

INTRODUCTION

The gram-negative aerobic bacterium *Pseudomonas aeruginosa* is ubiquitously present in soil, water, and vegetation, and is infectious to patients with cystic fibrosis, cancer, burns or compromised immune systems (Cross *et al.*, 1983). *Pseudomonas aeruginosa* often infects the lungs of patients with cystic fibrosis, where they form biofilms and become antibiotic resistant (Gaspar *et al.*, 2013). Like many other bacteria, *Pseudomonas aeruginosa* control these virulence properties by communicating with each other through quorum-sensing, by which the bacteria constitutively generate, release, detect and respond to small diffusible autoinducers (Miller and Bassler, 2001). The quorum-sensing molecule N-(3-oxododecanoyl)-L-homoserine lactone (C12) is produced by *Pseudomonas aeruginosa* to regulate bacterial LasI/rhlI and lasR/rhlR gene networks and influence bacterial intercellular communication (Hughes and Sperandio, 2008; Shiner *et al.*, 2005).

As a small, lipid-soluble, diffusible molecule, C12 readily enters various types of cells in the lungs of infected patients, including epithelial cells, endothelial cells, fibroblasts and leukocytes (Irie and Parsek, 2008; Rumbaugh, 2007; Schuster and Greenberg, 2006). The concentrations of C12 are believed to reach high micromolar levels in or adjacent to biofilms formed in the lung airways (Chambers *et al.*, 2005; Charlton *et al.*, 2000). C12 has been reported to alter many aspects of human airway epithelial cell physiology, including inhibition of proinflammatory cytokine secretion and activation of events commonly linked with apoptotic cell death, such as plasma membrane blebbing, cell shrinkage, nuclear condensation and fragmentation, caspase activation and mitochondrial membrane permeabilization (Fu *et al.*, 2007; Li *et al.*, 2004; Oliver *et al.*, 2009; Schwarzer *et al.*, 2010; Schwarzer *et al.*, 2012).

Upon C12 exposure, activation of diverse signaling pathways associated with apoptosis is observed in different mammalian cells. In breast carcinoma cells, C12 partially inhibits the Akt/PKB pathway, and the JAK/STAT pathway likely mediates pro-apoptotic activities of C12 (Li *et al.*, 2004). Similarly, C12 suppresses Akt activation by blocking Akt phosphorylation in undifferentiated intestinal epithelial cells, and overexpression of constitutively active Akt is capable of partially reducing C12 cytotoxicity (Taguchi *et al.*, 2014).

Signaling from the endoplasmic reticulum (ER) has also been implicated in apoptosis caused by C12. ER stress-responsive proteins inositol-requiring enzyme 1α (IRE1α) and X-Box Binding Protein 1 (XBP1) are required for C12-induced killing of mouse embryonic fibroblasts (MEF) (Valentine *et al.*, 2013). Furthermore, apoptosis-like morphological changes in the ER and mitochondria are observed in bone marrow-derived macrophages upon C12 treatment (Kravchenko *et al.*, 2006). Phosphorylation of p38 mitogen-activated protein kinase (MAPK) and eukaryotic translation initiation factor 2α (eIF2α) are two known biochemical markers that indicate cellular responses to C12.

Caspase activation is commonly observed in C12-exposed cells. Caspases are classified into two major categories: “initiator” caspases and “effector” caspases (Li and Yuan, 2008), and both of them are activated by C12. Serving as a marker for C12-triggered apoptosis,

activation of the effector caspase-3 has been detected in airway epithelial cells (Schwarzer *et al.*, 2012), fibroblasts (Schwarzer *et al.*, 2014a; Valentine *et al.*, 2013), intestinal epithelial cells (Taguchi *et al.*, 2014), breast carcinoma cells (Li *et al.*, 2004), lymphoma cells (Jacobi *et al.*, 2009), lung carcinoma cells (Zhao *et al.*, 2016), colorectal carcinoma cells (Zhao *et al.*, 2016), and leukocytes (Horikawa *et al.*, 2006; Kravchenko *et al.*, 2006; Tateda *et al.*, 2003). Activation of the "initiator" caspases caspase-8 (Jacobi *et al.*, 2009; Schwarzer *et al.*, 2012; Schwarzer *et al.*, 2014a; Tateda *et al.*, 2003) and caspase-9 (Kravchenko *et al.*, 2006; Schwarzer *et al.*, 2012) has also been reported. These data have suggested that both the extrinsic pathway initiated at the plasma membrane and the intrinsic pathway initiated in mitochondria may be activated.

However, the potential interplay between extrinsic and intrinsic pathways and "initiator" vs "effector" caspases in C12-activated apoptotic signaling remain unclear. In this paper, MEFs deficient in one or more caspases were investigated to elucidate the cell death signaling induced by C12. Our data indicate that C12 selectively triggers an apoptotic signaling pathway in which C12 appears to act by permeabilizing mitochondria, leading to activation of apoptosis.

RESULTS

Apoptosis is the major form of cell death caused by C12

In multicellular organisms, cell death is a highly heterogeneous process in which several distinct, in some cases partially overlapping, cell signaling cascades can be activated (Danial and Korsmeyer, 2004). Although C12's ability to trigger events commonly linked to apoptosis has been reported (Horikawa *et al.*, 2006; Li *et al.*, 2004; Schwarzer *et al.*, 2012; Schwarzer *et al.*, 2014a; Valentine *et al.*, 2013), it is unclear whether other cell death signaling is also involved. Caspase-3 and caspase-7 are two highly related "effector" caspases, and MEFs deficient in expression of both caspases are markedly resistant to both mitochondrial and death receptor-mediated apoptosis (Lakhani *et al.*, 2006). To characterize C12-induced signaling leading to cell death, we first investigated whether caspase-3 and caspase-7 were essential to mediate cytotoxic effects of C12. Cytotoxicity of C12 was examined in MEFs lacking caspase-3 (caspase-3-KO), caspase-7 (caspase-7-KO), or both (caspase-3/7-DKO) as well as their wild-type (WT) counterparts (Figure 1A). While C12-induced cell death was observed in wild-type, caspase-3-KO and caspase-7-KO MEFs, caspase-3/7-DKO MEFs were completely resistant to C12 exposure (Figure 1B). Moreover, less cell death was detected in caspase-3-KO or caspase-7-KO MEFs than their wild-type counterparts (Figure 1B). Since the levels of C12-induced cell death in caspase-3-KO-MEFs were lower than those observed in caspase-7-KO cells, caspase-3 appeared to play a more prominent role than caspase-7. Importantly, cleavage of caspase-3 and caspase-7, one of the hallmarks of apoptosis, was detected in wild-type MEFs treated with C12 (Figure 1C). Furthermore, PARP, a known substrate of caspase-3 and caspase-7, was also cleaved in wild-type MEFs upon C12 exposure, but not in their caspase-3/7-DKO counterparts. The essential role of caspase-3 and caspase-7 indicates that cell death induced by C12 is largely attributed to apoptosis.

C12-induced MOMP is independent of caspase-3 and caspase-7

Mitochondrial outer membrane permeabilization (MOMP) has been recognized to be a "no-return" step in both intrinsic and extrinsic apoptotic pathways (Newmeyer and Ferguson-Miller, 2003; Tait and Green, 2010). Two key events of MOMP are depolarization of mitochondrial membrane potential ($\Delta\psi_{mito}$) and release of cytochrome c from mitochondria into the cytosol. It is generally believed that MOMP occurs upstream of activation of caspase-3/7 (Newmeyer and Ferguson-Miller, 2003; Tait and Green, 2010). However, the involvement of caspase-3/7 activation in MOMP has been examined only for a limited number of apoptotic stimuli. In the study where caspase-3/7-DKO MEFs was first reported, UV irradiation evoked the apoptotic cascade by activating caspase-3/7 (Lakhani *et al.*, 2006). Unlike their wild-type counterparts, cells deficient in caspase-3/7 expression maintained their $\Delta\psi_{mito}$ upon UV irradiation, providing evidence that caspase-3/7 regulated the initial phase of MOMP in certain apoptotic paradigms.

To explore C12-initiated apoptotic signaling, we studied the involvement of caspase-3/7 in both $\Delta\psi_{mito}$ depolarization and cytochrome c release. Depolarization of $\Delta\psi_{mito}$ was evaluated by determining the changes in fluorescence with the voltage-dependent dye JC1 being released from mitochondria into the cytosol and nucleus. Within minutes of C12 exposure, mitochondrial $\Delta\psi_{mito}$ in wild-type MEFs became almost completely depolarized to a level close to the maximal depolarization induced by the ionophore carbonyl cyanide-p-trifluoromethoxyphenylhydrazone FCCP (Figure 2A), consistent with studies in other cell types (Schwarzer *et al.*, 2012; Schwarzer *et al.*, 2014a; Zhao *et al.*, 2016). Importantly, C12 triggered similar degrees of $\Delta\psi_{mito}$ depolarization in both wild-type and caspase-3/7-DKO MEFs (Figure 2B), indicating that MOMP induced by C12 occurs upstream of "effector" caspase activation.

Furthermore, immunofluorescence studies were used to evaluate C12-evoked redistribution of cytochrome c from mitochondria to the cytosol and nuclei. As shown in representative images of both wild-type and caspase-3/7-DKO MEFs under control conditions, cytochrome c and the mitochondrial outer membrane protein Tom20 exhibited overlapping punctate and perinuclear distribution that is typical of mitochondrial morphology (Figure 3A). In addition, nuclei displayed characteristic oval shape with smooth boundaries that largely excluded cytochrome c and Tom20. Upon C12 treatment, distribution of cytochrome c was diffuse in the cytosol and nuclei in both wild-type and caspase-3/7-DKO MEFs, whereas Tom20 maintained its perinuclear distribution, demonstrating that mitochondria in wild-type and caspase-3/7-DKO MEFs were permeabilized with cytochrome c released into the cytosol and diffused into the nuclei. The redistribution of cytochrome c was quantitated by calculating the punctate/diffuse index. These quantitative measurements showed that C12 caused equivalent cytochrome c release in wild-type and caspase-3/7-DKO MEFs (Figure 3B), while Tom20 was still localized in mitochondria in the presence of C12 (Figure 3C).

Next, the levels of cytochrome c in the cytosol of MEFs exposed to C12 were determined by a biochemical fractionation approach (Adlam *et al.*, 2005; Childs *et al.*, 2002; Wang *et al.*, 2011). Whole cell extracts and the cytosolic fractions from wild-type and caspase-3/7-DKO MEFs with or without exposure to C12 were acquired. The absence of Tom20 in the cytosolic fractions under all conditions indicated that the cytosolic fractions were free of

mitochondria (Figure 3D). Importantly, C12 increased the amounts of cytochrome c in the cytosolic fractions of wild-type and caspase-3/7-DKO MEFs to the similar levels (Figure 3E). Thus, immunofluorescence and biochemical fractionation data were consistent in showing that C12 caused cytochrome c release from mitochondria into the cytosol regardless of caspase-3/7 expression. Overall, these results provide more evidence that C12 triggers MOMP independent of caspase-3 and caspase-7 activation.

C12-induced apoptosis is independent of caspase-8

The “initiator” caspase-8 mediates extrinsic pathway initiated at the plasma membrane, whereas the “initiator” caspase-9 is responsible for the mitochondria-dependent intrinsic pathway (Li and Yuan, 2008). Activation of extrinsic and intrinsic apoptosis pathways has been reported in cells treated with C12, but it is not clear to what degree each pathway contributes to cell death (Jacobi *et al.*, 2009; Schwarzer *et al.*, 2012; Schwarzer *et al.*, 2014b; Tateda *et al.*, 2003). To systematically investigate which apoptotic pathway is involved, we first examined MEFs deficient in caspase-8 and their wild-type counterparts (Supplementary figure 1A). Consistent with previous reports (Beisner *et al.*, 2005; Moujalled *et al.*, 2012), MEFs lacking caspase-8 were resistant to the combined treatment of recombinant human TNF-α protein and the Smac mimetic TL-32711 (Supplementary figure 1B). Upon treatment with C12, similar levels of cell death (Figure 4A) and caspase-3/7 enzymatic activities (Figure 4B) were detected in both wild-type and caspase-8-KO MEFs. It was discovered that caspase-7 expression level in these particular wild-type MEFs was very low compared with that in corresponding caspase-8-KO MEFs (Figure 4C). While C12 triggered cleavage of caspase-3 and caspase-7 in caspase-8-KO MEFs, only cleavage of caspase-3 was observed in wild-type cells, likely due to the lack of caspase-7 expression. With more caspase-3 cleaved in wild-type MEFs exposed to C12, higher levels of caspase-7 activation were detected in C12-treated caspase-8-KO MEFs. Similar levels of PARP cleavage was observed in both wild-type and caspase-8-KO MEFs, in agreement with the cell death data (Figure 4A).

To validate the role of caspase-8 in C12-induced cell death, caspase-8 expression was stably reduced in human colorectal carcinoma cell line HCT116 and human pancreatic carcinoma cell line PANC-1 by shRNA (Supplementary figures 2A and 2D). As expected, HCT116 and PANC-1 cells with reduced caspase-8 expression exhibited resistance to the combined treatment of TNF-α and the protein synthesis inhibitor cycloheximide (Supplementary figures 2B and 2E). In contrast, C12 caused similar levels of cell death in both HCT116 and PANC-1 cells regardless of caspase-8 expression (Supplementary figures 2C and 2F), providing more evidence that C12 induces apoptosis independent of caspase-8.

To further investigate the role of caspase-8 in C12-initiated apoptotic signaling, we studied the involvement of caspase-8 in depolarization of $\Delta\psi_{mito}$ induced by C12. Consistent with its effects on cell viability and caspase-3/7 activation, deficiency in caspase-8 expression did not affect the ability of C12 to induce rapid depolarization of $\Delta\psi_{mito}$ (Figures 4D–E). These data indicate that caspase-8-mediated extrinsic pathway dose not play a pivotal role in C12-induced apoptosis.

C12 primarily triggers mitochondria-dependent intrinsic apoptosis pathway

Next, we investigated whether the “initiator” caspase-9 was responsible for C12-induced apoptosis. For this purpose, MEFs lacking caspase-9 expression and corresponding wild-type MEFs were examined (Supplementary figure 3A). Chemotherapeutic drugs etoposide and actinomycin D, two stimuli known to evoke mitochondria-dependent intrinsic apoptosis pathway, induced cell death in wild-type but not in caspase-9-KO MEFs (Supplementary figures 3B–C). Unlike their wild-type counterparts, MEFs deficient in caspase-9 were completely resistant to C12 treatment (Figure 5A). Importantly, C12 failed to evoke any caspase-3/7 enzymatic activities in MEFs lacking caspase-9 expression (Figure 5B). Furthermore, cleavage of caspase-3 and caspase-7 was only observed in wild-type MEFs treated with C12, but not in caspase-9-KO MEFs (Figure 5C). Importantly, reexpressing caspase-9 in caspase-9-KO MEFs sensitized the cells to C12 (Supplementary figure 4).

To further examine the involvement of caspase-9 in C12-indcued apoptosis, caspase-9 expression in human pancreatic carcinoma cell line MIA PaCa-2 was stably decreased by shRNA (Supplementary figure 5A). MIA PaCa-2 cells with reduced caspase-9 expression were resistant to C12 treatment (Supplementary figure 5B). APAF1 plays a key role in intrinsic apoptotic signaling by forming oligomeric apoptosomes along with cytochrome c released into the cytosol, which leads to subsequent activation of caspase-9 (Shakeri *et al.*, 2017). Deficiency in APAF1 expression rendered MEFs completely resistant to C12 exposure (Supplementary figure 6). Overall, these data suggest that C12 induces apoptotic signaling largely through activating the mitochondria-dependent intrinsic apoptotic pathway.

C12-induced MOMP is independent of caspase-9

It has been discovered that many apoptotic stimuli induce MOMP, leading to cytochrome c release, apoptosome assembly and subsequent caspase-9 activation (Newmeyer and Ferguson-Miller, 2003; Tait and Green, 2010). However, emerging evidence suggests that caspase-9 activation also plays a role in MOMP in some apoptosis paradigms. For instance, it has been shown that reducing caspase-9 expression or inhibiting caspase-9 activity is able to block depolarization of $\Delta\psi_{mito}$ (Eeva *et al.*, 2009; Guerrero *et al.*, 2012; Hakem *et al.*, 1998; Samraj *et al.*, 2006; Samraj *et al.*, 2007). To clarify the roles of caspase-9 in MOMP mediated by C12, $\Delta\psi_{mito}$ was measured in wild-type and caspase-9-KO MEFs. Contrary to its effects on cell viability and caspase-3/7 activation (Figure 5), deficiency in caspase-9 expression did not affect the ability of C12 to induce rapid depolarization of $\Delta\psi_{mito}$ (Figure 6), indicating that caspase-9 was not involved in C12-induced MOMP.

To further validate this notion, we examined cytochrome c redistribution from mitochondria to the cytosol and nuclei upon C12 exposure using immunofluorescence staining. While C12 evoked the release of cytochrome c from mitochondria to the cytosol and nuclei regardless of caspase-9 expression, Tom20 maintained perinuclear distribution following C12 treatment (Figures 7A–C). Moreover, C12-induced subcellular redistribution of cytochrome c in wild-type and caspase-9-KO MEFs was examined using a biochemical fractionation approach. Isolated cytosolic fractions were not contaminated with mitochondria, evident by the absence of Tom20 in those fractions (Figure 7D). C12 induced equivalent redistribution of cytochrome c from mitochondria to the cytosol in wild-type and caspase-9-KO MEFs

(Figure 7E). Thus, immunofluorescence microscopy and biochemical fractionation data have demonstrated that C12 evokes cytochrome c release from mitochondria into the cytosol regardless of caspase-9 expression. Taken together, these data indicate that C12 causes acute MOMP independent of any "initiator" caspase, suggesting that the effects of C12 on MOMP might be attributed to its direct action on mitochondria.

C12 directly induces MOMP *in vitro*

Since C12 depolarized $\Delta\psi_{mito}$ starting within 1 minute and achieving complete effect within 10–20 minutes independent of both "initiator" caspases and "effector" caspases (Figures 2, 4 and 6), we reasoned that C12 could possess activities that directly permeabilize mitochondria. To this purpose, we examined the effects of C12 on mitochondrial outer membrane integrity *in vitro*. Mitochondria isolated from wild-type MEFs were exposed to DMSO (control) or to 30 or 300 μM C12. We assessed the amount of cytochrome c released from mitochondria using western blot analysis (Figure 8A). In a manner dependent on C12 concentrations, less cytochrome c was detected in mitochondrial fractions, with concomitant increase of cytochrome c in released fractions (Figure 8B). Furthermore, C12's ability to cause cytochrome c release *in vitro* reached its maximal level within 20 minutes of incubation, consistent with the time frame of depolarization of $\Delta\psi_{mito}$ in cells (Supplementary figure 7). These data indicate that C12 is able to permeabilize mitochondria directly *in vitro*. Overall, our data suggest that C12 evokes a mitochondrial apoptotic signaling pathway in which C12 directly permeabilizes mitochondria, leading to activation of apoptosis (Figure 8C).

DISCUSSION

The quorum-sensing molecule C12 evokes apoptosis in a variety of mammalian cells (Fu *et al.*, 2007; Li *et al.*, 2004; Oliver *et al.*, 2009; Schwarzer *et al.*, 2010; Schwarzer *et al.*, 2012). Several signaling pathways leading to apoptosis have been associated with C12 cytotoxicity. In addition to activating the intrinsic apoptosis pathway, C12 has also been shown to activate caspase-8, implicating a role of the extrinsic apoptotic cascade in C12-induced apoptosis (Jacobi *et al.*, 2009; Schwarzer *et al.*, 2012; Schwarzer *et al.*, 2014a; Tateda *et al.*, 2003). One possible scenario is that C12 functions as a ligand that is recognized by receptors on the plasma membrane. However, the interplay between the intrinsic and extrinsic pathways as well as the functions of key molecules involved had not been clearly elucidated previously. In this study we present evidence that caspase-3/7 and caspase-9 but not caspase-8 are essential for C12-induced apoptotic cell death in fibroblasts, indicating that C12 selectively triggers the mitochondria-dependent intrinsic apoptotic pathway. Therefore, the events associated with activating a plasma membrane receptor are likely secondary responses to MOMP at least in fibroblasts. However, it is possible that in other cell types intrinsic and extrinsic pathways might be equally involved or one pathway plays a more prominent role in mediating C12-induced apoptosis. The dispensable roles of both the "initiator" caspases and "effector" caspases in C12-indcued MOMP suggest that C12 may exert its pro-apoptotic effect without the involvement of signaling upstream of mitochondria.

Several signaling pathways linked to apoptosis initiation, including JAK/STAT (Li *et al.*, 2004), MAPK and eIF2α pathways (Kravchenko *et al.*, 2006) have been implicated in C12-evoked cell death. In breast carcinoma cells, C12 induces apoptosis by partially inhibiting the Akt/PKB pathway and abolishing STAT3 activity (Li *et al.*, 2004). These apoptosis-associated signaling pathways are normally involved in multiple steps of signal transduction, and the biological events reflective of these signaling cascades are largely observed hours following C12 incubation. In contrast, depolarization of $\Delta\psi_{mito}$, the earliest step of MOMP (Chipuk and Green, 2008; Goldstein *et al.*, 2000), is always detected within minutes following C12 exposure and reaches its maximal levels in 20 minutes (Figures 2, 4 and 6; also see (Schwarzer *et al.*, 2012; Schwarzer *et al.*, 2014b; Schwarzer *et al.*, 2015; Zhao *et al.*, 2016)). Therefore, Akt/PKB pathway and STAT3 signaling are unlikely responsible for C12-indcued depolarization of $\Delta\psi_{mito}$. In a variety of mammalian cell types, phosphorylation of eIF2α and p38 MAPK has been observed 5 minutes following C12 treatment. It has been shown that eIF2α phosphorylation induces apoptosis through activating the unfolded protein responses (Holcik and Sonenberg, 2005), which does not appear to be accountable for the quick effect of C12 on depolarization of $\Delta\psi_{mito}$. Likewise, apoptosis triggered by p38 MAPK phosphorylation is largely attributed to phosphorylation and modulation of anti- and pro-apoptotic Bcl-2 proteins (Cai *et al.*, 2006; Grethe *et al.*, 2004). Previous studies indicate that C12 evokes depolarization of $\Delta\psi_{mito}$ independent of both anti- and pro-apoptotic Bcl-2 proteins in various cellular systems (Schwarzer *et al.*, 2014a; Zhao *et al.*, 2016). Thus, it is unlikely that MAPK signaling is directly involved in C12-mediated depolarization of $\Delta\psi_{mito}$. Overall, it appears that activation of JAK/STAT, eIF2a and MAPK signaling pathways may be secondary to MOMP initiation in C12-triggered apoptosis cascade.

ER stress-induced apoptosis is a well-described cellular process, which is associated with the compromise of ER membrane permeability to luminal Ca^{2+} and proteins as well as activation of ER-specific caspase-12 and probably downstream caspase-9 (Mekahli *et al.*, 2011; Morishima *et al.*, 2002; Nakagawa *et al.*, 2000; Wang *et al.*, 2011). C12 has been demonstrated to trigger the ER stress pathway (Horke *et al.*, 2015; Schwarzer *et al.*, 2012; Schwarzer *et al.*, 2015; Valentine *et al.*, 2013). Release of ER Ca^{2+} into the cytosol is observed within minutes of C12 exposure, which is implicated in C12-induced apoptosis (Horke *et al.*, 2015; Schwarzer *et al.*, 2012; Schwarzer *et al.*, 2015). Since the effects of ER stress on $\Delta\psi_{mito}$ occurs several hours following ER Ca^{2+} pool depletion (Wang *et al.*, 2011), the likelihood that C12-induced ER Ca^{2+} release directly causes depolarization of $\Delta\psi_{mito}$ is low. Furthermore, recent research indicates that ER stress-mediated apoptosis requires the pro-apoptotic Bcl-2 proteins Bak and Bax to permeabilize mitochondria (Wang *et al.*, 2011; Wei *et al.*, 2001; Zong *et al.*, 2003), which is inconsistent with the evidence that C12 triggers depolarization of $\Delta\psi_{mito}$ independent of Bak and Bax in various cellular systems (Schwarzer *et al.*, 2014a; Zhao *et al.*, 2016). Thus, it is unlikely that ER stress signaling is directly involved in C12-mediated depolarization of $\Delta\psi_{mito}$. Conceivably, C12 or its metabolite(s) acts directly on mitochondria and permeabilizes them. In support of this notion, our *in vitro* studies demonstrate that C12 directly permeabilizes mitochondria (Figure 8). These data suggest that C12 directly affects mitochondrial outer membrane integrity probably by physically inserting into the membrane or interacting with mitochondrial protein(s) that serves as C12 receptor(s).

As a lactone, C12 is known to be hydrolyzed into a carboxylic acid *in vitro* by paraoxonase 2 (PON2), an enzyme with lactonase and arylesterase activities (Draganov *et al.*, 2005). Intracellular PON2 has been demonstrated to hydrolyze C12 and cause subsequent intracellular acidification, which is thought to mediate biological responses to C12, such as triggering stress signaling (Horke *et al.*, 2015). However, the association between C12-evoked intracellular acidification and depolarization of $\Delta\psi_{mito}$ remains unclear. Our previous studies have demonstrated that PON2 promotes C12-induced apoptosis in various cellular systems (Schwarzer *et al.*, 2015; Tao *et al.*, 2016; Zhao *et al.*, 2016). C12 fails to induce MOMP in MEFs lacking PON2 expression, showing that C12 alone is insufficient to trigger MOMP but requires expression of PON2 (Schwarzer *et al.*, 2015). In addition to its localization on the ER membrane and plasma membrane (Hagmann *et al.*, 2014), PON2 has also been shown to reside in mitochondria (Devarajan *et al.*, 2011). One possibility is that PON2 cleaves C12 into a pro-apoptotic metabolite(s) that permeabilizes mitochondria. A previous study reports that a C12 derivative with its lactone ring broken open exhibits little cytotoxicity when incubated with the cultured cells, suggesting that the structural integrity of C12 lactone ring is essential for C12-evoked apoptosis (Kravchenko *et al.*, 2006). However, it is unclear whether the carboxylic acid derivative of C12 is able to pass through the plasma membrane to enter cells as easily as C12. Another possible scenario is that C12 or a PON2-mediated derivative might also react with other molecules (e.g. phosphorylation) in cells to generate secondary metabolite(s) with stronger pro-apoptotic activities. Alternatively, PON2 has anti-oxidant properties that modulate peroxidation of membrane lipids (Hagmann *et al.*, 2014) and may regulate intracellular lipid biogenesis (Meilin *et al.*, 2010; Rosenblat *et al.*, 2009), which might affect mitochondrial outer membrane lipid composition in such a way that C12 preferentially inserts into mitochondria.

Whatever the molecular details of C12 action on mitochondria, our study has shown that C12 induces a unique apoptotic signaling pathway in which C12 or C12 metabolite(s) acts as a mitolytic molecule that directly permeabilizes mitochondria, releasing cytochrome c to activate caspase-9, caspase-3/7 and subsequent downstream apoptosis cascade.

EXPERIMENTAL PROCEDURES

Reagents

N-(3-oxododecanoyl)-homoserine lactone (C12), cycloheximide, etoposide and actinomycin D were purchased from Sigma (St. Louis, MO). Propidium iodide (PI) was obtained from Thermo (Waltham, MA). Recombinant human TNF-α was purchased from Peprotech (Rocky Hill, NJ). The Smac mimetic TL-32711 was purchased from Active Biochem (Maplewood, NJ). Unless otherwise stated, all reagents were dissolved in dimethyl sulfoxide (DMSO). C12 was dissolved in DMSO to generate a stock solution of 100 mM, which was aliquoted and stored at −20°C. Before applied to the cells, C12 was diluted to various concentrations in the appropriate medium or buffer with the final concentration of 0.2% DMSO, unless otherwise stated. Dulbecco's Modified Eagle's Medium (DMEM), penicillin/streptomycin, trypsin, and L-glutamine were obtained from Mediatech (Manassas, VA), and fetal bovine serum (FBS) was purchased from Gemini (Broderick, CA). Caspase-Glo assay 3/7 kit was purchased from Promega (Madison, WI). Antibodies (Abs) used for western blot

analysis were anti-β-actin mAb (Sigma), anti-full-length-caspase-3 pAb; anti-full-length-caspase-7 pAb; anti-full-length-caspase-8 pAb; anti-full-length-caspase-9 pAb; anti-cleaved-caspase-3 pAb; anti-cleaved-caspase-7 pAb; anti-PARP pAb (Cell signaling; Danvers, MA), anti-cytochrome c mAb for western blot (Santa Cruz; Dallas, TX), anti-cytochrome c mAb for immunofluorescence staining (BD Transduction Laboratory; San Jose, CA), anti-Tom40 pAb; anti-SOD2 pAb (Santa Cruz), anti-Tom20 pAb (a gift from Dr. Brian Wattenberg), anti-APAF1 pAb (Abcam; Cambridge, MA), peroxidase-conjugated goat anti-mouse IgG (Thermo), peroxidase-conjugated goat anti-rabbit IgG (Thermo), AlexaFluor488-conjugated goat anti-mouse IgG (Thermo), AlexaFluor594-conjugated goat anti-rabbit IgG (Thermo).

Cell lines and cell culture

Immortalized mouse embryonic fibroblasts (MEFs) deficient in the expression of caspase-8 and their wild-type counterparts were provided by Professor David Vaux (Walter and Eliza Hall Institute of Medical Research, Parkville, VIC Australia). MEFs lacking caspase-9 and their wild-type counterparts were obtained from Professor Jerry Adams (Walter and Eliza Hall Institute of Medical Research). MEFs lacking caspase-3, caspase-7, caspase-3 and caspase-7, or their wild-type counterparts were obtained from Professor Richard Flavell (Yale University). Primary MEFs deficient in APAF1 and their wild-type counterparts were provided by Professor Tak Mak (University Health Network, Toronto, Canada). Human colorectal carcinoma HCT116, human pancreatic carcinoma PANC-1 and human pancreatic carcinoma MIA PaCa-2 were purchased from ATCC (Manassas, VA). To generate HCT116 and PANC-1 cells with reduced caspase-8 expression or vector control, cells were first infected by caspase-8 shRNA lentiviral particles or control shRNA lentiviral particles (Santa Cruz) with 10 μg/ml polybrene. Stable cells were obtained by culturing the cells in the medium with 5 μg/ml puromycin. Similarly, MIA PaCa-2 cells with stably decreased caspase-9 expression or vector control were acquired by infection with caspase-9 shRNA lentiviral particles or control shRNA lentiviral particles (Santa Cruz) in the presence of 10 μg/ml polybrene and 5 μg/ml puromycin. The lentivrial plasmid expressing murine caspase-9 (pReceiver-Lv105-murine-caspase-9) and its empty vector control were purchased from GeneCopoeia (Rockville, MD). To acquire MEFs reexpressing caspase-9 or vector control, caspase-9-KO MEFs cells were infected by caspase-9 lentiviral particles or control lentiviral particles with 5 μg/ml polybrene and 5 μg/ml puromycin in the medium. All of the cell lines were grown and maintained in DMEM supplemented with 10% FBS, 100 units/ml penicillin, and 100 μg/ml streptomycin. Cells were all cultured in a 5% CO_2 humidified incubator at 37°C.

Cell death assays

The indicated cells were plated in a 48-well tissue culture plate with 10,000 cells in each well and cultured for 24 hours. Unless otherwise stated, medium containing 0.2% DMSO with or without the indicated agents was incubated with the cells. Following treatment with the indicated agents, cells were harvested in the presence of 1 μg/ml propidium iodide (PI). Cell viability was measured by PI exclusion using flow cytometry (FACScalibur, Beckon Dickinson; San Jose, CA). The percentage of cell death was determined as100 minus the value of cell viability measurement.

Caspase-3/7 activity

Caspase-3/7 activities were measured using a Caspase-Glo assay kit (Promega, Madison, WI). In this assay, the proluminescent substrate containing the amino acid sequence Asp-Glu-Val-Asp (DEVD) is cleaved by activated caspase-3/7, resulting in the release of a luciferase substrate (aminoluciferin) and the production of luminescent signal. 24 hours before the treatment, cells were plated in white-walled 96-well plates. At the indicated time points following treatment with various agents, cells were mixed with CellTiter-Glo reagent, and luminescence was quantified by a Gemini EM microplate spectrofluorometer (Molecular Devices; Sunnyvale, CA) according to the manufacturer's protocol. Data were presented as relative luminescence units (RLUs).

Western blot analysis

Equal amounts of proteins (30 μg) were separated on a 4–12% Bis-Tris gel (Bio-Rad; Hercules, CA) and transferred onto PVDF membrane (Millipore; Billerica, MA). The membrane was incubated with appropriate primary or secondary antibodies either overnight at 4°C or at room temperature for 3 hours in 1X phosphate-buffered saline (PBS) containing 5% (w/v) nonfat dry milk (Bio-Rad) and 0.2% (v/v) Tween 20. Protein levels were detected using the enhanced chemiluminescent detection system (Thermo) as described previously (Zhao *et al.*, 2015).

Measuring $\Delta\psi_{mito}$ using imaging microscopy of JC1

For imaging experiments to measure mitochondrial membrane potential ($\Delta\psi_{mito}$), cells were incubated with growth media containing the $\Delta\psi_{mito}$ probe JC1 (10 μM) for 10 minutes at room temperature, and then washed three times with Ringer's solution to remove the extra dye. JC1-loaded cells were placed onto a chamber on the stage of a Nikon Diaphot inverted microscope. Cells were maintained at room temperature during the course of the experiments. Treatments were made by diluting stock solutions into Ringer's solution at the concentrations stated in the text. Fluorescence imaging evaluation of $\Delta\psi_{mito}$ was carried out using equipment and methods that have been reported previously (Schwarzer *et al.*, 2014a; Zhao *et al.*, 2016). Briefly, a Nikon Diaphot inverted microscope with a Fluor 20 X objective (0.75 numerical aperture) was used. A charge coupled device camera acquired JC1 emission images (green: 510–540 nm; red: 580–620 nm) during excitation at 490 +/− 5 nm using filter wheels (Lambda-10, Sutter Instruments; Novato, CA). Axon Imaging Workbench 5.1 (Axon Instruments; Foster City, CA) controlled filters and collection of data. Images were corrected for background using regions without cells. In cells under control conditions, mitochondria displayed red and green fluorescence of JC1. C12 induced-depolarization of $\Delta\psi_{mito}$ resulted in a decrease in JC1 red fluorescence and an increase in JC1 green fluorescence. The protonophore FCCP caused maximal depolarization of $\Delta\psi_{mito}$ with JC1 red fluorescence decreasing to very low levels and JC1 green fluorescence reaching maximal levels. All green / red JC1 fluorescence ratios were normalized to minimal JC1 ratios obtained at the beginning of each experiment and maximal JC1 ratios acquired following 10 μM FCCP treatment at the end of each experiment: Normalized JC1 Ratio = (ratio at a given time - minimal ratio recorded at the start) / (maximal ratio obtained with FCCP - minimal ratio recorded at the start) * 100%. For time course experiments (shown in Figures 2A, 4D, and

6A) an initial red/green JC1 ratio baseline was recorded before the addition of 50 μM C12. After JC1 ratios reached a stable plateau, 10 μM FCCP was added to achieve maximal mitochondrial membrane depolarization (= Max JC1 ratio). Normalized JC1 ratios at plateau (before FCCP treatment) from at least three different experiments have been averaged for summary graphs (shown in Figures 2B, 4E, and 6B).

Immunofluorescence microscopy

MEFs plated onto cover glasses 24 hours earlier were rinsed with Ringer's solution and incubated for 4 hours with either vehicle (DMSO) or 50 μM C12 in Ringer's solution. The immunofluorescence staining of cytochrome c and Tom20 were carried out as described previously (Zhao *et al.*, 2016). Images were captured using a Nikon Eclipse Ti confocal microscope (Nikon; Melville, NY) equipped with a PlanApo 60x, 1.42 NA oil immersion objective. To minimize variability for quantitative assessment, the same microscope settings were used across vehicle control and C12-treated samples for three individual experiments. Fields of view were captured to acquire a sample size of at least 100 cells for each individual experiment. Intracellular distribution of cytochrome c and Tom20 was analyzed using ImageJ (NIH). Cytochrome c release from mitochondria was quantified by determining the standard deviation (SD) of the average pixel intensity (brightness) of cytochrome c signals in the image of individual cells – this is named as the punctate/diffuse index following an established protocol (Bouchier-Hayes *et al.*, 2008; Goldstein *et al.*, 2000; Goldstein *et al.*, 2005; Munoz-Pinedo *et al.*, 2006; Wang *et al.*, 2011). Briefly, when cytochrome c is highly localized within mitochondria, it will display a punctate distribution pattern, leading to high SD of the average pixel intensity, but when cytochrome c is distributed throughout the cell, the SD will be low. Therefore, a decrease in the SD (punctate/diffuse index) is an index of cytochrome c redistribution from mitochondria to the cytosol.

Subcellular fractionation

MEFs ($4 \times 10^{\wedge 6}$) were plated onto 15-cm tissue culture dishes for 24 hours and washed with Ringer's solution and cultured for 4 hours with either vehicle (DMSO) or 50 μM C12 in Ringer's solution. Subcellular fractionation was carried out as described previously with some modification (Wang *et al.*, 2011). MEFs were collected and washed with 1 × PBS, and resuspended in 200 μl buffer containing 5 mM Tris-HCl (pH 7.5), 210 mM mannitol, 70 mM sucrose, and 1 mM EDTA and protease inhibitors (Complete, Roche Diagnostics; Indianapolis, IN). The cells were broken open by passing through a homogenizer. The whole cell lysate was centrifuged at 400 × g using a Sorvall Legend RT centrifuge (Thermo) for 10 minutes at 4 °C to eliminate large cellular debris and nuclei. The supernatants were centrifuged in a TLA 100.2 rotor using a TL-100 tabletop ultracentrifuge (Beckman; Fullerton, CA) at 10,000 × g for 10 minutes at 4 °C. The supernatants were subsequently centrifuged at 350,000 × g for 2 hours at 4 °C to obtain the cytosolic fractions. Protein concentrations in the isolated fractions were evaluated by BCA assays (Thermo). Equivalent amounts of whole cell extract and the cytosolic fractions (5 μg) were electrophoresed. The presence of cytochrome c, Tom20 and actin was detected by western blot. The protein intensity was determined using ImageJ software (NIH). To normalize sample loading variation, the relative levels of cytochrome c in the whole cell extracts and the cytosolic fractions were first calculated by dividing the cytochrome c value into the corresponding

value for actin. The normalized values of cytochrome c levels in the cytosolic fractions were calculated as a percentage of relative cytochrome c levels in the corresponding whole cell extracts.

Detection of the release of cytochrome c from mitochondria *in vitro*

Mitochondria were purified from MEFs as described previously (25). Isolated mitochondria were resuspended in buffer containing 12 mM HEPES (pH 7.5), 1.7 mM Tris-HCl (pH 7.5), 100 mM KCl, 140 mM mannitol, 23 mM sucrose, 2 mM KH_2PO_4, 1 mM $MgCl_2$, 0.67 mM EGTA, and 0.6 mM EDTA supplemented with protease inhibitors (Complete; Roche Diagnostics, Indianapolis, IN). After one hour incubation with C12 at 30°C, mitochondrial vesicles were centrifuged at 10,000×g for 10 min and then dissolved in 1×SDS-PAGE loading buffer. Proteins in the supernatant and pellet fractions were detected by Western blotting.

Statistical analysis

All experiments were performed at least three times. Results are presented as mean ± standard deviation. Statistical analysis was performed using Student's two tail t-test. A p value < 0.05 was considered significant.

Supplementary Material

Refer to Web version on PubMed Central for supplementary material.

Acknowledgments

We are grateful to Dr. John Eaton (University of Louisville) for critical reading of the paper, Dr. David Vaux (Walter and Eliza Hall Institute of Medical Research) for providing wild-type and caspase-8-KO MEFs, Dr. Jerry Adams (Walter and Eliza Hall Institute of Medical Research) for providing MEFs lacking caspase-9 and their wild-type counterparts, Dr. Richard Flavell (Yale University) for providing MEFs lacking caspase-3, caspase-7, caspase-3 and caspase-7 and their wild-type counterparts, Dr. Tak Mak (University Health Network) for providing MEFs lacking APAF1 and their wild-type counterparts. This work was supported by grants from National Institutes of Health CA106599, CA175003, and RR018733, a pilot project funded through the 1P30GM106396 Molecular Targets Phase III CoBRE grant, a Research Initiation Grant from University of Louisville and funding from the James Graham Brown Cancer Center (CL) and grants from National Institutes of Health PN2-EY-018241 and Cystic Fibrosis Research, Inc. New Horizons (TM). This work was also funded by CAS Pioneer Hundred Talents Program (GZ).

ABBREVIATIONS LIST

C12	N-(3-oxododecanoyl)-homoserine lactone
ER	endoplasmic reticulum
MEF	mouse embryonic fibroblasts
IRE1α	inositol-requiring enzyme 1α
XBP1	X-Box Binding Protein 1
eIF2α	eukaryotic translation initiation factor 2α
MOMP	mitochondrial outer membrane permeabilization

WT	wild-type
$\Delta\psi_{mito}$	mitochondrial membrane potential
FCCP	carbonyl cyanide-p-trifluoromethoxyphenylhydrazone
PON2	paraoxonase 2

References

Adlam VJ, Harrison JC, Porteous CM, James AM, Smith RA, Murphy MP, et al. Targeting an antioxidant to mitochondria decreases cardiac ischemia-reperfusion injury. FASEB J. 2005; 19:1088–1095. [PubMed: 15985532]

Beisner DR, Ch'en IL, Kolla RV, Hoffmann A, Hedrick SM. Cutting edge: innate immunity conferred by B cells is regulated by caspase-8. J Immunol. 2005; 175:3469–3473. [PubMed: 16148088]

Bouchier-Hayes L, Munoz-Pinedo C, Connell S, Green DR. Measuring apoptosis at the single cell level. Methods. 2008; 44:222–228. [PubMed: 18314052]

Cai B, Chang SH, Becker EB, Bonni A, Xia Z. p38 MAP kinase mediates apoptosis through phosphorylation of BimEL at Ser-65. J Biol Chem. 2006; 281:25215–25222. [PubMed: 16818494]

Chambers CE, Visser MB, Schwab U, Sokol PA. Identification of N-acylhomoserine lactones in mucopurulent respiratory secretions from cystic fibrosis patients. FEMS Microbiol Lett. 2005; 244:297–304. [PubMed: 15766782]

Charlton TS, de NR, Netting A, Kumar N, Hentzer M, Givskov M, et al. A novel and sensitive method for the quantification of N-3-oxoacyl homoserine lactones using gas chromatography-mass spectrometry: application to a model bacterial biofilm. Environ Microbiol. 2000; 2:530–541. [PubMed: 11233161]

Childs AC, Phaneuf SL, Dirks AJ, Phillips T, Leeuwenburgh C. Doxorubicin treatment in vivo causes cytochrome C release and cardiomyocyte apoptosis, as well as increased mitochondrial efficiency, superoxide dismutase activity, and Bcl-2:Bax ratio. Cancer Res. 2002; 62:4592–4598. [PubMed: 12183413]

Chipuk JE, Green DR. How do BCL-2 proteins induce mitochondrial outer membrane permeabilization? Trends Cell Biol. 2008; 18:157–164. [PubMed: 18314333]

Cross A, Allen JR, Burke J, Ducel G, Harris A, John J, et al. Nosocomial infections due to Pseudomonas aeruginosa: review of recent trends. Rev Infect Dis. 1983; 5(Suppl 5):S837–S845. [PubMed: 6361960]

Danial NN, Korsmeyer SJ. Cell death: critical control points. Cell. 2004; 116:205–219. [PubMed: 14744432]

Devarajan A, Bourquard N, Hama S, Navab M, Grijalva VR, Morvardi S, et al. Paraoxonase 2 deficiency alters mitochondrial function and exacerbates the development of atherosclerosis. Antioxid Redox Signal. 2011; 14:341–351. [PubMed: 20578959]

Draganov DI, Teiber JF, Speelman A, Osawa Y, Sunahara R, La Du BN. Human paraoxonases (PON1, PON2, and PON3) are lactonases with overlapping and distinct substrate specificities. J Lipid Res. 2005; 46:1239–1247. [PubMed: 15772423]

Eeva J, Nuutinen U, Ropponen A, Matto M, Eray M, Pellinen R, et al. Feedback regulation of mitochondria by caspase-9 in the B cell receptor-mediated apoptosis. Scand J Immunol. 2009; 70:574–583. [PubMed: 19906200]

Fu Z, Bettega K, Carroll S, Buchholz KR, Machen TE. Role of Ca2+ in responses of airway epithelia to Pseudomonas aeruginosa, flagellin, ATP, and thapsigargin. Am J Physiol Lung Cell Mol Physiol. 2007; 292:L353–L364. [PubMed: 16963531]

Gaspar MC, Couet W, Olivier JC, Pais AA, Sousa JJ. Pseudomonas aeruginosa infection in cystic fibrosis lung disease and new perspectives of treatment: a review. Eur J Clin Microbiol Infect Dis. 2013; 32:1231–1252. [PubMed: 23619573]

Goldstein JC, Munoz-Pinedo C, Ricci JE, Adams SR, Kelekar A, Schuler M, et al. Cytochrome c is released in a single step during apoptosis. Cell Death Differ. 2005; 12:453–462. [PubMed: 15933725]

Goldstein JC, Waterhouse NJ, Juin P, Evan GI, Green DR. The coordinate release of cytochrome c during apoptosis is rapid, complete and kinetically invariant. Nat Cell Biol. 2000; 2:156–162. [PubMed: 10707086]

Grethe S, Ares MP, Andersson T, Porn-Ares MI. p38 MAPK mediates TNF-induced apoptosis in endothelial cells via phosphorylation and downregulation of Bcl-x(L). Exp Cell Res. 2004; 298:632–642. [PubMed: 15265709]

Guerrero AD, Schmitz I, Chen M, Wang J. Promotion of Caspase Activation by Caspase-9-mediated Feedback Amplification of Mitochondrial Damage. J Clin Cell Immunol. 2012; 3

Hagmann H, Kuczkowski A, Ruehl M, Lamkemeyer T, Brodesser S, Horke S, et al. Breaking the chain at the membrane: paraoxonase 2 counteracts lipid peroxidation at the plasma membrane. FASEB J. 2014; 28:1769–1779. [PubMed: 24421402]

Hakem R, Hakem A, Duncan GS, Henderson JT, Woo M, Soengas MS, et al. Differential requirement for caspase 9 in apoptotic pathways in vivo. Cell. 1998; 94:339–352. [PubMed: 9708736]

Holcik M, Sonenberg N. Translational control in stress and apoptosis. Nat Rev Mol Cell Biol. 2005; 6:318–327. [PubMed: 15803138]

Horikawa M, Tateda K, Tuzuki E, Ishii Y, Ueda C, Takabatake T, et al. Synthesis of Pseudomonas quorum-sensing autoinducer analogs and structural entities required for induction of apoptosis in macrophages. Bioorg Med Chem Lett. 2006; 16:2130–2133. [PubMed: 16460931]

Horke S, Xiao J, Schutz EM, Kramer GL, Wilgenbus P, Witte I, et al. Novel Paraoxonase 2-Dependent Mechanism Mediating the Biological Effects of the Pseudomonas aeruginosa Quorum-Sensing Molecule N-(3-Oxo-Dodecanoyl)-L-Homoserine Lactone. Infect Immun. 2015; 83:3369–3380. [PubMed: 26056385]

Hughes DT, Sperandio V. Inter-kingdom signalling: communication between bacteria and their hosts. Nat Rev Microbiol. 2008; 6:111–120. [PubMed: 18197168]

Irie Y, Parsek MR. Quorum sensing and microbial biofilms. Curr Top Microbiol Immunol. 2008; 322:67–84. [PubMed: 18453272]

Jacobi CA, Schiffner F, Henkel M, Waibel M, Stork B, Daubrawa M, et al. Effects of bacterial N-acyl homoserine lactones on human Jurkat T lymphocytes-OdDHL induces apoptosis via the mitochondrial pathway. Int J Med Microbiol. 2009; 299:509–519. [PubMed: 19464950]

Kravchenko VV, Kaufmann GF, Mathison JC, Scott DA, Katz AZ, Wood MR, et al. N-(3-oxo-acyl)homoserine lactones signal cell activation through a mechanism distinct from the canonical pathogen-associated molecular pattern recognition receptor pathways. J Biol Chem. 2006; 281:28822–28830. [PubMed: 16893899]

Lakhani SA, Masud A, Kuida K, Porter GA Jr, Booth CJ, Mehal WZ, et al. Caspases 3 and 7: key mediators of mitochondrial events of apoptosis. Science. 2006; 311:847–851. [PubMed: 16469926]

Li J, Yuan J. Caspases in apoptosis and beyond. Oncogene. 2008; 27:6194–6206. [PubMed: 18931687]

Li L, Hooi D, Chhabra SR, Pritchard D, Shaw PE. Bacterial N-acylhomoserine lactone-induced apoptosis in breast carcinoma cells correlated with down-modulation of STAT3. Oncogene. 2004; 23:4894–4902. [PubMed: 15064716]

Meilin E, Aviram M, Hayek T. Paraoxonase 2 (PON2) decreases high glucose-induced macrophage triglycerides (TG) accumulation, via inhibition of NADPH-oxidase and DGAT1 activity: studies in PON2-deficient mice. Atherosclerosis. 2010; 208:390–395. [PubMed: 19748094]

Mekahli D, Bultynck G, Parys JB, De SH, Missiaen L. Endoplasmic-reticulum calcium depletion and disease. Cold Spring Harb Perspect Biol. 2011; 3

Miller MB, Bassler BL. Quorum sensing in bacteria. Annu Rev Microbiol. 2001; 55:165–199. [PubMed: 11544353]

Morishima N, Nakanishi K, Takenouchi H, Shibata T, Yasuhiko Y. An endoplasmic reticulum stress-specific caspase cascade in apoptosis. Cytochrome c-independent activation of caspase-9 by caspase-12. J Biol Chem. 2002; 277:34287–34294. [PubMed: 12097332]

Moujalled DM, Cook WD, Lluis JM, Khan NR, Ahmed AU, Callus BA, et al. In mouse embryonic fibroblasts, neither caspase-8 nor cellular FLICE-inhibitory protein (FLIP) is necessary for TNF to activate NF-kappaB, but caspase-8 is required for TNF to cause cell death, and induction of FLIP by NF-kappaB is required to prevent it. Cell Death Differ. 2012; 19:808–815. [PubMed: 22095280]

Munoz-Pinedo C, Guio-Carrion A, Goldstein JC, Fitzgerald P, Newmeyer DD, Green DR. Different mitochondrial intermembrane space proteins are released during apoptosis in a manner that is coordinately initiated but can vary in duration. Proc Natl Acad Sci U S A. 2006; 103:11573–11578. [PubMed: 16864784]

Nakagawa T, Zhu H, Morishima N, Li E, Xu J, Yankner BA, et al. Caspase-12 mediates endoplasmic-reticulum-specific apoptosis and cytotoxicity by amyloid-beta. Nature. 2000; 403:98–103. [PubMed: 10638761]

Newmeyer DD, Ferguson-Miller S. Mitochondria: releasing power for life and unleashing the machineries of death. Cell. 2003; 112:481–490. [PubMed: 12600312]

Oliver CM, Schaefer AL, Greenberg EP, Sufrin JR. Microwave synthesis and evaluation of phenacylhomoserine lactones as anticancer compounds that minimally activate quorum sensing pathways in Pseudomonas aeruginosa. J Med Chem. 2009; 52:1569–1575. [PubMed: 19260689]

Rosenblat M, Coleman R, Reddy ST, Aviram M. Paraoxonase 2 attenuates macrophage triglyceride accumulation via inhibition of diacylglycerol acyltransferase 1. J Lipid Res. 2009; 50:870–879. [PubMed: 19091699]

Rumbaugh KP. Convergence of hormones and autoinducers at the host/pathogen interface. Anal Bioanal Chem. 2007; 387:425–435. [PubMed: 16912860]

Samraj AK, Keil E, Ueffing N, Schulze-Osthoff K, Schmitz I. Loss of caspase-9 provides genetic evidence for the type I/II concept of CD95-mediated apoptosis. J Biol Chem. 2006; 281:29652–29659. [PubMed: 16895904]

Samraj AK, Sohn D, Schulze-Osthoff K, Schmitz I. Loss of caspase-9 reveals its essential role for caspase-2 activation and mitochondrial membrane depolarization. Mol Biol Cell. 2007; 18:84–93. [PubMed: 17079734]

Schuster M, Greenberg EP. A network of networks: quorum-sensing gene regulation in Pseudomonas aeruginosa. Int J Med Microbiol. 2006; 296:73–81. [PubMed: 16476569]

Schwarzer C, Fu Z, Morita T, Whitt AG, Neely AM, Li C, et al. Paraoxonase 2 serves a proapopotic function in mouse and human cells in response to the Pseudomonas aeruginosa quorum-sensing molecule N-(3-Oxododecanoyl)-homoserine lactone. J Biol Chem. 2015; 290:7247–7258. [PubMed: 25627690]

Schwarzer C, Fu Z, Patanwala M, Hum L, Lopez-Guzman M, Illek B, et al. Pseudomonas aeruginosa biofilm-associated homoserine lactone C12 rapidly activates apoptosis in airway epithelia. Cell Microbiol. 2012; 14:698–709. [PubMed: 22233488]

Schwarzer C, Fu Z, Shuai S, Babbar S, Zhao G, Li C, et al. Pseudomonas aeruginosa homoserine lactone triggers apoptosis and Bak/Bax-independent release of mitochondrial cytochrome C in fibroblasts. Cell Microbiol. 2014a; 16:1094–1104. [PubMed: 24438098]

Schwarzer C, Ravishankar B, Patanwala M, Shuai S, Fu Z, Illek B, et al. Thapsigargin blocks Pseudomonas aeruginosa homoserine lactone-induced apoptosis in airway epithelia. Am J Physiol Cell Physiol. 2014b; 306:C844–C855. [PubMed: 24598360]

Schwarzer C, Wong S, Shi J, Matthes E, Illek B, Ianowski JP, et al. Pseudomonas aeruginosa Homoserine lactone activates store-operated cAMP and cystic fibrosis transmembrane regulator-dependent Cl- secretion by human airway epithelia. J Biol Chem. 2010; 285:34850–34863. [PubMed: 20739289]

Shakeri R, Kheirollahi A, Davoodi J. Apaf-1: Regulation and function in cell death. Biochimie. 2017; 135:111–125. [PubMed: 28192157]

Shiner EK, Rumbaugh KP, Williams SC. Inter-kingdom signaling: deciphering the language of acyl homoserine lactones. FEMS Microbiol Rev. 2005; 29:935–947. [PubMed: 16219513]

Taguchi R, Tanaka S, Joe GH, Maseda H, Nomura N, Ohnishi J, et al. Mucin 3 is involved in intestinal epithelial cell apoptosis via N-(3-oxododecanoyl)-L-homoserine lactone-induced suppression of Akt phosphorylation. Am J Physiol Cell Physiol. 2014; 307:C162–C168. [PubMed: 24848113]

Tait SW, Green DR. Mitochondria and cell death: outer membrane permeabilization and beyond. Nat Rev Mol Cell Biol. 2010; 11:621–632. [PubMed: 20683470]

Tao S, Luo Y, Bin H, Liu J, Qian X, Ni Y, et al. Paraoxonase 2 modulates a proapoptotic function in LS174T cells in response to quorum sensing molecule N-(3-oxododecanoyl)-L-homoserine lactone. Sci Rep. 2016; 6:28778. [PubMed: 27364593]

Tateda K, Ishii Y, Horikawa M, Matsumoto T, Miyairi S, Pechere JC, et al. The Pseudomonas aeruginosa autoinducer N-3-oxododecanoyl homoserine lactone accelerates apoptosis in macrophages and neutrophils. Infect Immun. 2003; 71:5785–5793. [PubMed: 14500500]

Valentine CD, Anderson MO, Papa FR, Haggie PM. X-box binding protein 1 (XBP1s) is a critical determinant of Pseudomonas aeruginosa homoserine lactone-mediated apoptosis. PLoS Pathog. 2013; 9:e1003576. [PubMed: 23990788]

Wang X, Olberding KE, White C, Li C. Bcl-2 proteins regulate ER membrane permeability to luminal proteins during ER stress-induced apoptosis. Cell Death Differ. 2011; 18:38–47. [PubMed: 20539308]

Wei MC, Zong WX, Cheng EH, Lindsten T, Panoutsakopoulou V, Ross AJ, et al. Proapoptotic BAX and BAK: a requisite gateway to mitochondrial dysfunction and death. Science. 2001; 292:727–730. [PubMed: 11326099]

Zhao G, Lu H, Li C. Proapoptotic activities of protein disulfide isomerase (PDI) and PDIA3 protein, a role of the Bcl-2 protein Bak. J Biol Chem. 2015; 290:8949–8963. [PubMed: 25697356]

Zhao G, Neely AM, Schwarzer C, Lu H, Whitt AG, Stivers NS, et al. N-(3-oxo-acyl) homoserine lactone inhibits tumor growth independent of Bcl-2 proteins. Oncotarget. 2016; 7:5924–5942. [PubMed: 26758417]

Zong WX, Li C, Hatzivassiliou G, Lindsten T, Yu QC, Yuan J, et al. Bax and Bak can localize to the endoplasmic reticulum to initiate apoptosis. J Cell Biol. 2003; 162:59–69. [PubMed: 12847083]

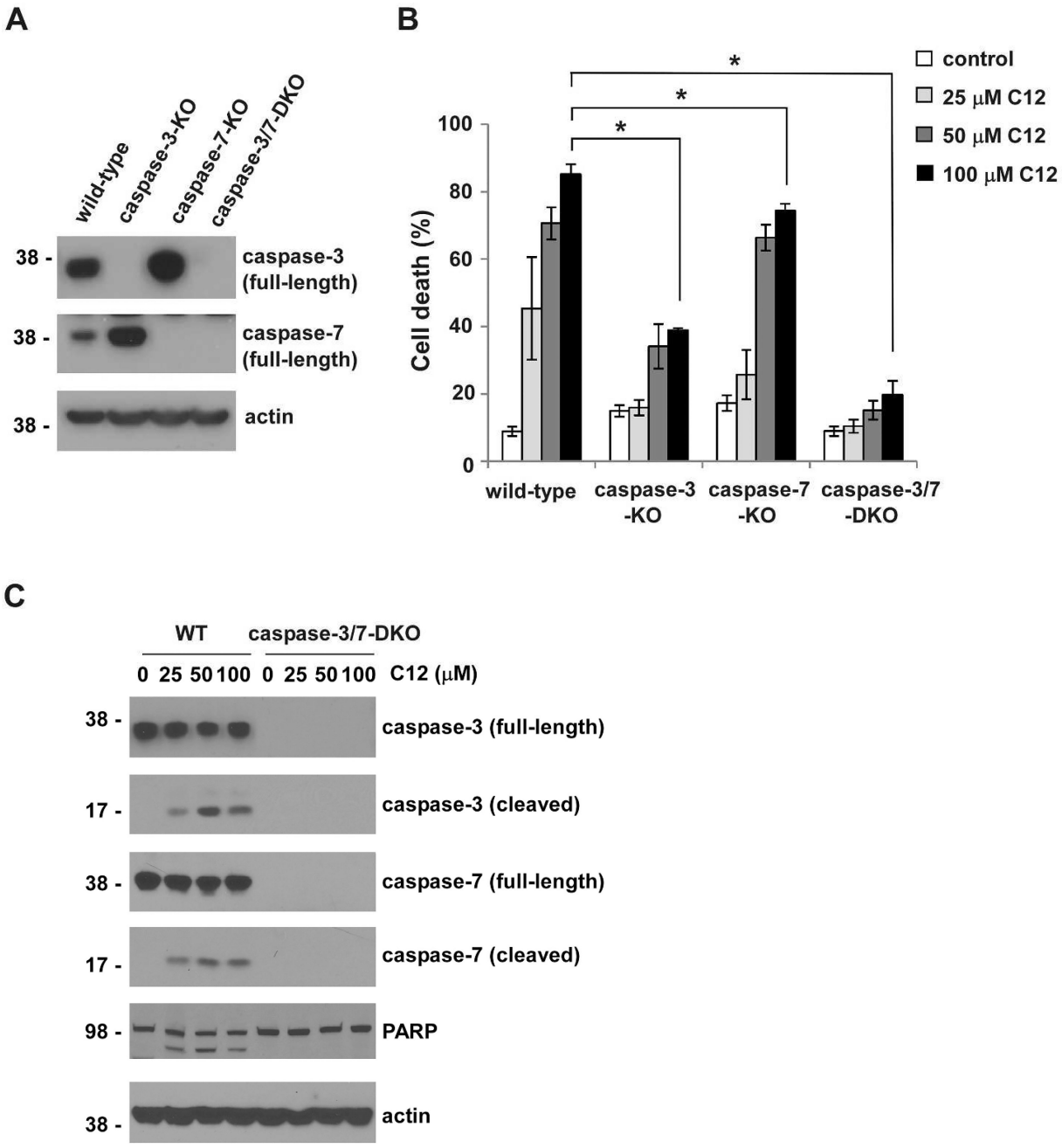

Figure 1. Caspase-3 and caspase-7 are essential for C12-induced apoptosis

(A) The expression of caspase-3 and caspase-7 in the indicated MEFs was examined by western blot. The molecular weight markers are labeled on the left (kD). **(B)** MEFs were treated with C12 for 48 hours, and cell viability was measured by propidium iodide exclusion. All data are presented as means ± standard deviations of three independent experiments with duplicate samples measured in each independent experiment. Asterisks indicate $P < 0.05$ (*); Student's unpaired t test. **(C)** Cleavage of caspase-3 and caspase-7 was determined by western blot. Whole cell extracts of wild-type (WT) and caspase-3/7-DKO

MEFs were acquired following 16 hour-treatment of C12. The data shown is typical of three independent experiments. The molecular weight markers are labeled on the left (kD).

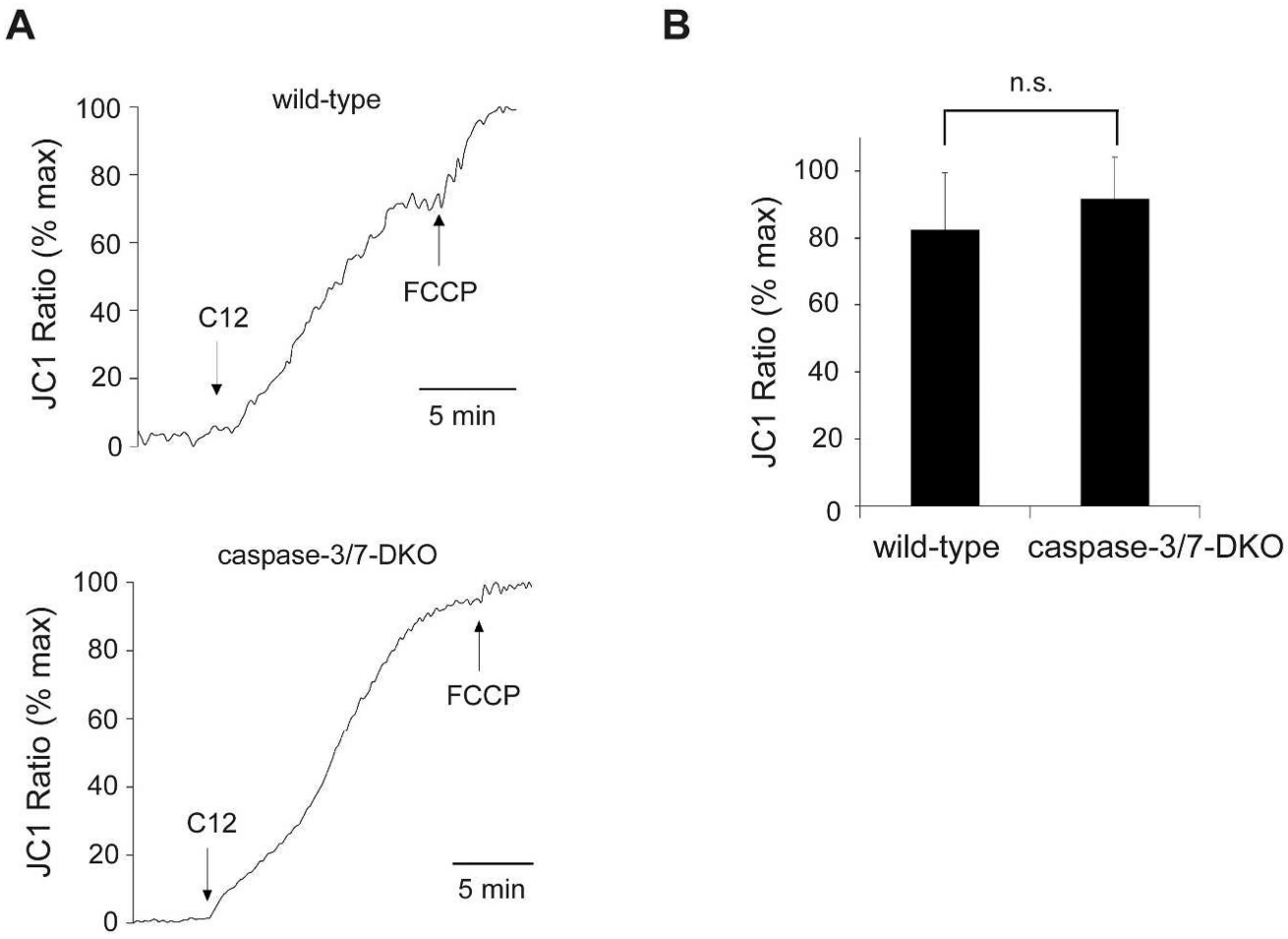

Figure 2. Caspase-3 and caspase-7 are not required for mitochondrial depolarization induced by C12

(A) MEFs from wild-type and caspase-3/7-DKO mice were loaded with the mitochondrial potential dye JC1, and fluorescence was measured using imaging microscopy during sequential treatment with 50 μM C12 and 10 μM FCCP. JC1 fluorescence increase (equivalent to depolarization of $\Delta\psi_{mito}$) was observed in both cell lines upon C12 exposure. The data are plotted as the percentage of maximal JC1 fluorescence increase caused by FCCP. Typical results from three independent experiments are shown. **(B)** Addition of C12 caused equivalent depolarization of $\Delta\psi_{mito}$ in wild-type and caspase-3/7-DKO MEFs. The data shown in (A) were summarized. The magnitude of steady-state depolarization of $\Delta\psi_{mito}$ induced by C12 was normalized as the percentage of the value of maximal depolarization of $\Delta\psi_{mito}$ caused by FCCP. All data are shown as means ± standard deviations of three independent experiments. Student's unpaired t test. ns, no significance.

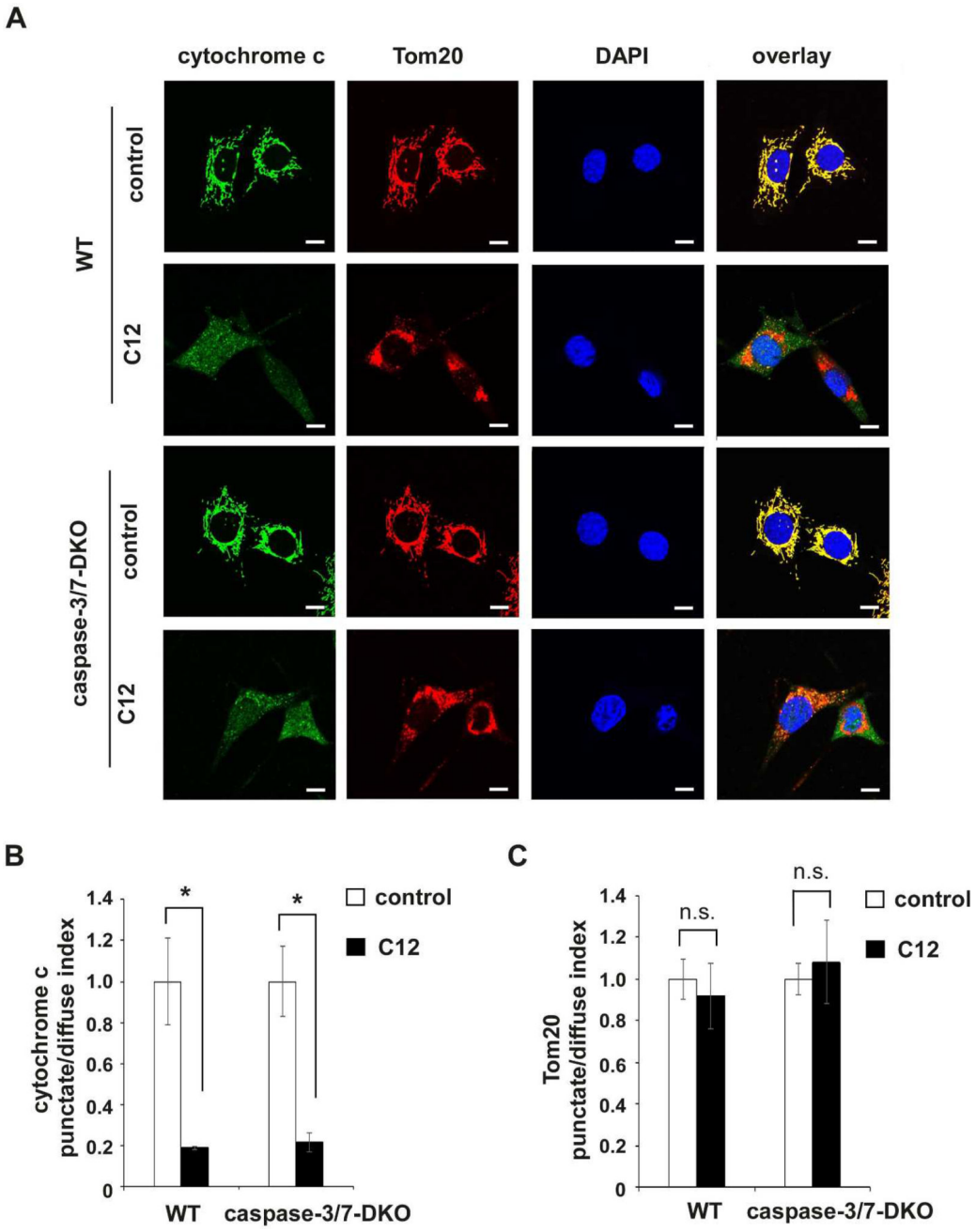

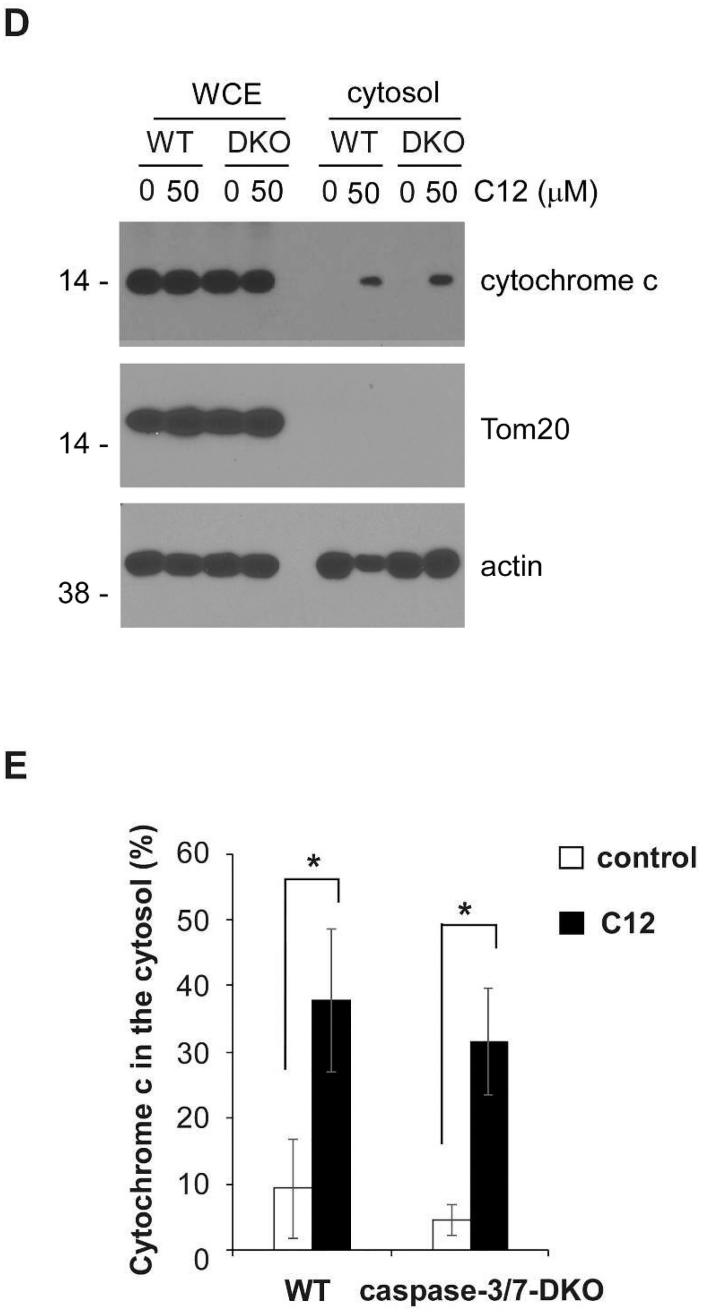

Figure 3. C12-induced mitochondrial outer membrane permeabilization occurs upstream of caspase-3/7 activation

(A) Representative confocal images of MEFs treated with either DMSO (control) or 50 μM C12 for 4 hours (typical of three independent experiments). The mitochondrial marker Tom20 is shown in red, cytochrome c in green, and DAPI in blue. Following treatment with C12, staining of cytochrome c became diffuse and lost its co-localization with Tom20. WT, wild-type. Scale bar, 10 μm. **(B–C)** The intracellular distribution of cytochrome c (B) and Tom20 (C) was evaluated by determining the punctate/diffuse index, defined as the standard deviation of the mean pixel intensity of cytochrome c or Tom20 staining for each cell. Summary data show the means ± standard deviations of the punctuate/diffuse index

calculated from three independent experiments with more than 100 cells in each independent experiment. Asterisks indicate $P < 0.05$ (*), ns, no significance. Student's unpaired t test. **(D)** Following incubation with either DMSO or 50 μM C12 for 4 hours, WT or caspase-3/7-DKO MEFs were fractionated, and the cytosolic fractions were obtained. The amounts of cytochrome c, Tom20 and actin in the whole cell extracts (WCE) and the cytosolic fractions were determined by western blot (typical of three independent experiments). The molecular weight markers are labeled on the left (kD). DKO, caspase-3/7-DKO. **(E)** The summary of normalized cytochrome c levels in the cytosolic fractions shown in (D). The intensities of cytochrome c, Tom20 and actin were quantified using ImageJ software (NIH). As described in Materials and Methods, the normalized values of cytochrome c levels in the cytosolic fractions were calculated as a percentage of relative cytochrome c levels in the corresponding whole cell extracts. The data are shown as means ± standard deviations of three independent experiments. Asterisks indicate $P < 0.05$ (*); Student's unpaired t test.

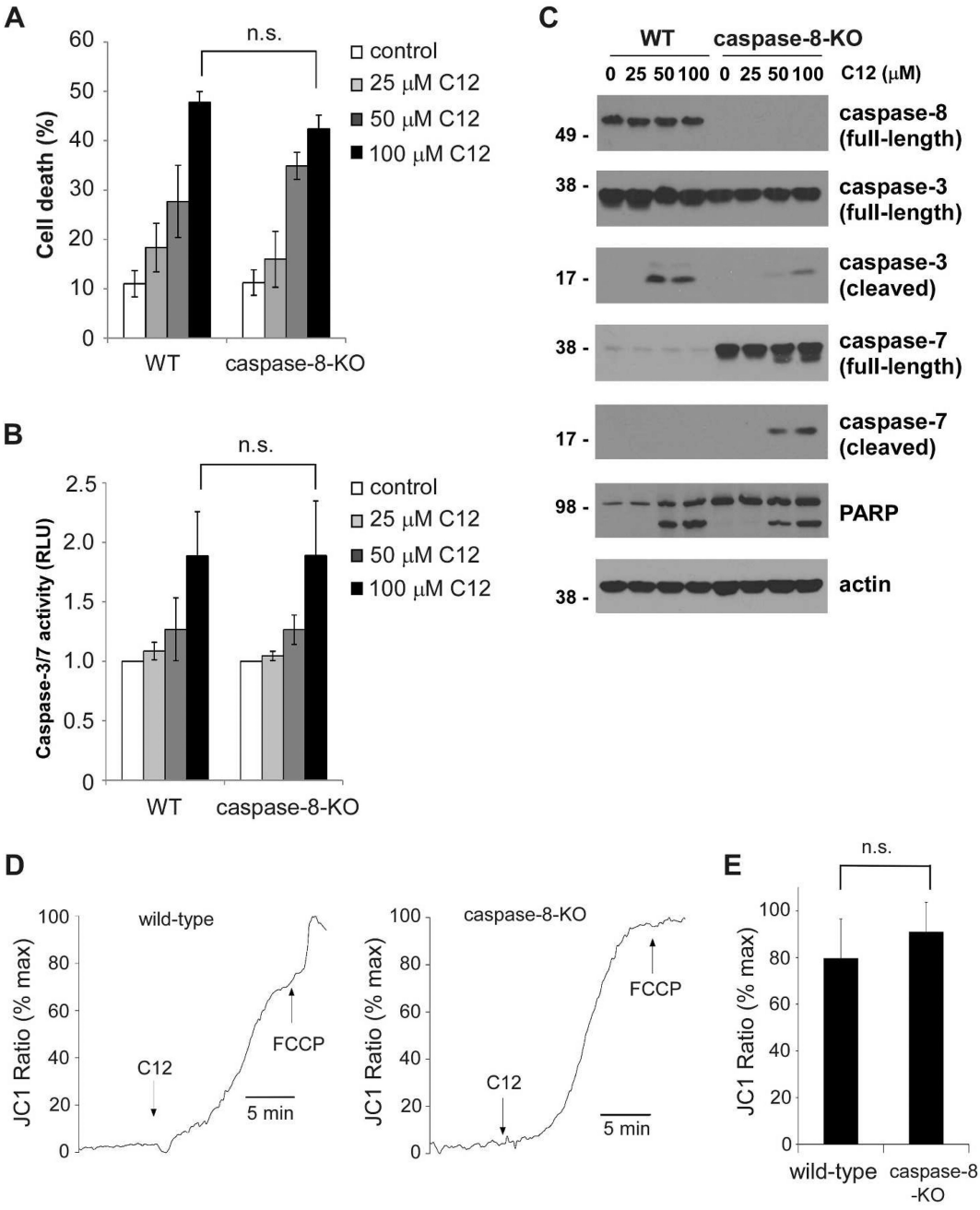

Figure 4. Caspase-8 activation is not involved in C12-induced apoptosis

(A) The cytotoxicity of C12 on wild-type (WT) and caspase-8-KO MEFs was assessed 24 hours after treatment. Data are presented as means ± standard deviations of three independent experiments with duplicate samples measured in each independent experiment. **(B)** Caspase-3/7 activities were evaluated 24 hours after C12 treatment. Data are shown as means ± standard deviations of three independent experiments with duplicate samples measured in each independent experiment. **(C)** Upon the treatment of C12 for 12 hours, cleavage of caspase-3 and caspase-7 in WT and caspase-8-KO MEFs was evaluated by western blot. The data shown are typical of three independent experiments. The molecular

weight markers are labeled on the left (kD). **(D)** Mitochondrial membrane potentials of WT and caspase-8-KO MEFs loaded with JC1 were determined by fluorescence microscopy upon treatment with 50 μM C12 and 10 μM FCCP. The increase in JC1 fluorescence was equivalent to depolarization of $\Delta\psi_{mito}$, which was observed in both WT and caspase-8-KO MEFs upon C12 exposure. The data are normalized as the percentage of maximal JC1 fluorescence increase evoked by FCCP. Typical results from three independent experiments are shown. **(E)** C12 caused equivalent mitochondrial depolarization in WT and caspase-8-KO MEFs. The summary of the data shown in (D) is presented. The value of steady-state depolarization of $\Delta\psi_{mito}$ caused by C12 in WT and caspase-8-KO MEFs was plotted as the percentage of the value of maximal depolarization of $\Delta\psi_{mito}$ caused by FCCP. Data are presented as means ± standard deviations of three independent experiments. ns, no significance. Student's unpaired t test.

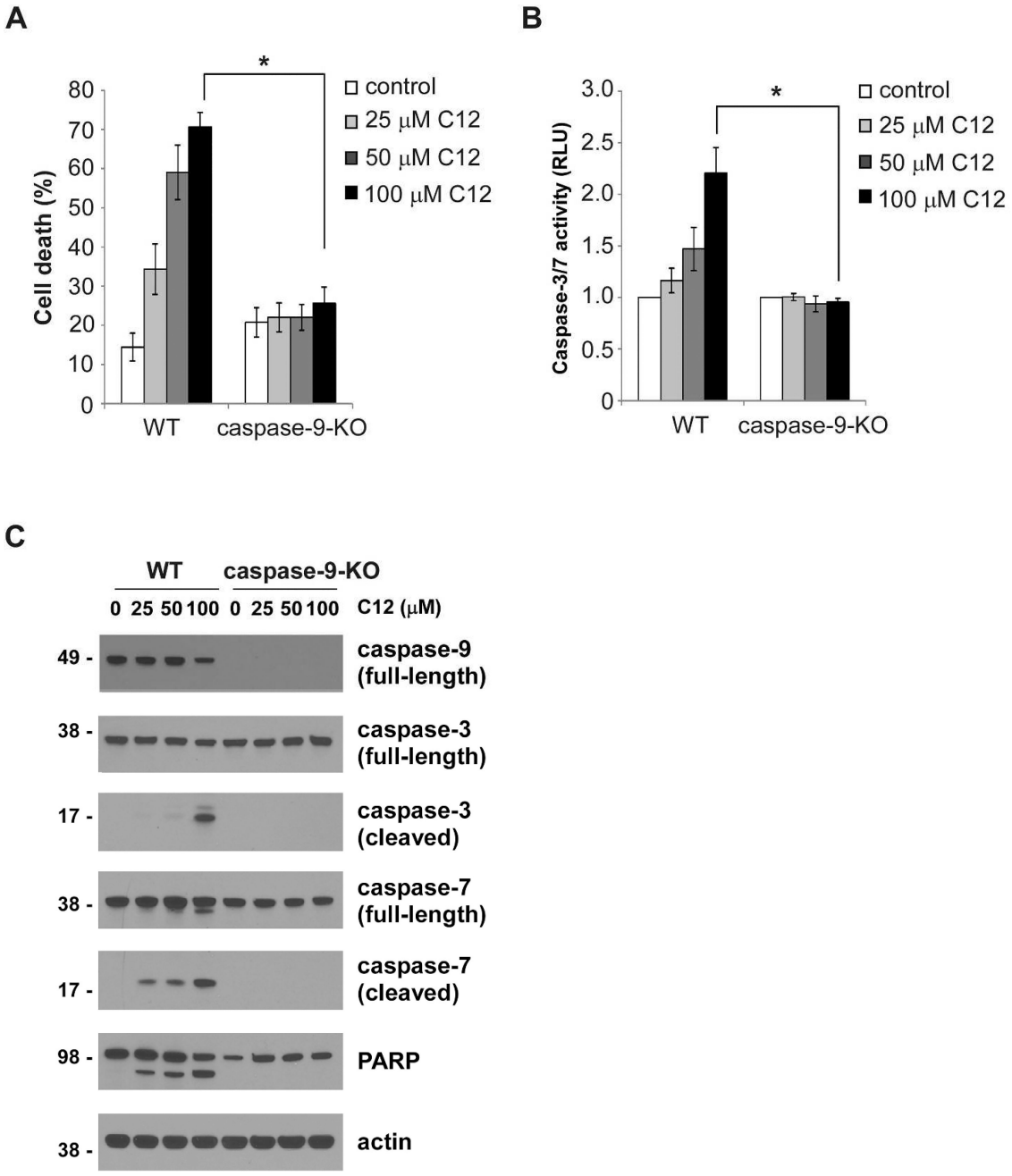

Figure 5. C12-induced apoptosis is dependent on caspase-9

(A) Cell viabilities of wild-type (WT) and caspase-9-KO MEFs were measured 48 hours after treatment with different doses of C12. The data are shown as means ± standard deviations of three independent experiments with duplicate samples measured in each independent experiment. Asterisks indicate $P < 0.05$ (*), Student's unpaired t test. **(B)** Caspase-3/7 activities were determined for wild-type and caspase-9-KO MEFs treated with different doses of C12 for 24 hours. The data are means ± standard deviations of three independent experiments with duplicate samples measured in each independent experiment. Asterisks indicate $P < 0.05$ (*), Student's unpaired t test. **(C)** Cleavage of caspase-3 and

caspase-7 was evaluated by western blot following 16 hour-exposure of C12. The data are typical of three independent experiments. The molecular weight markers are labeled on the left (kD).

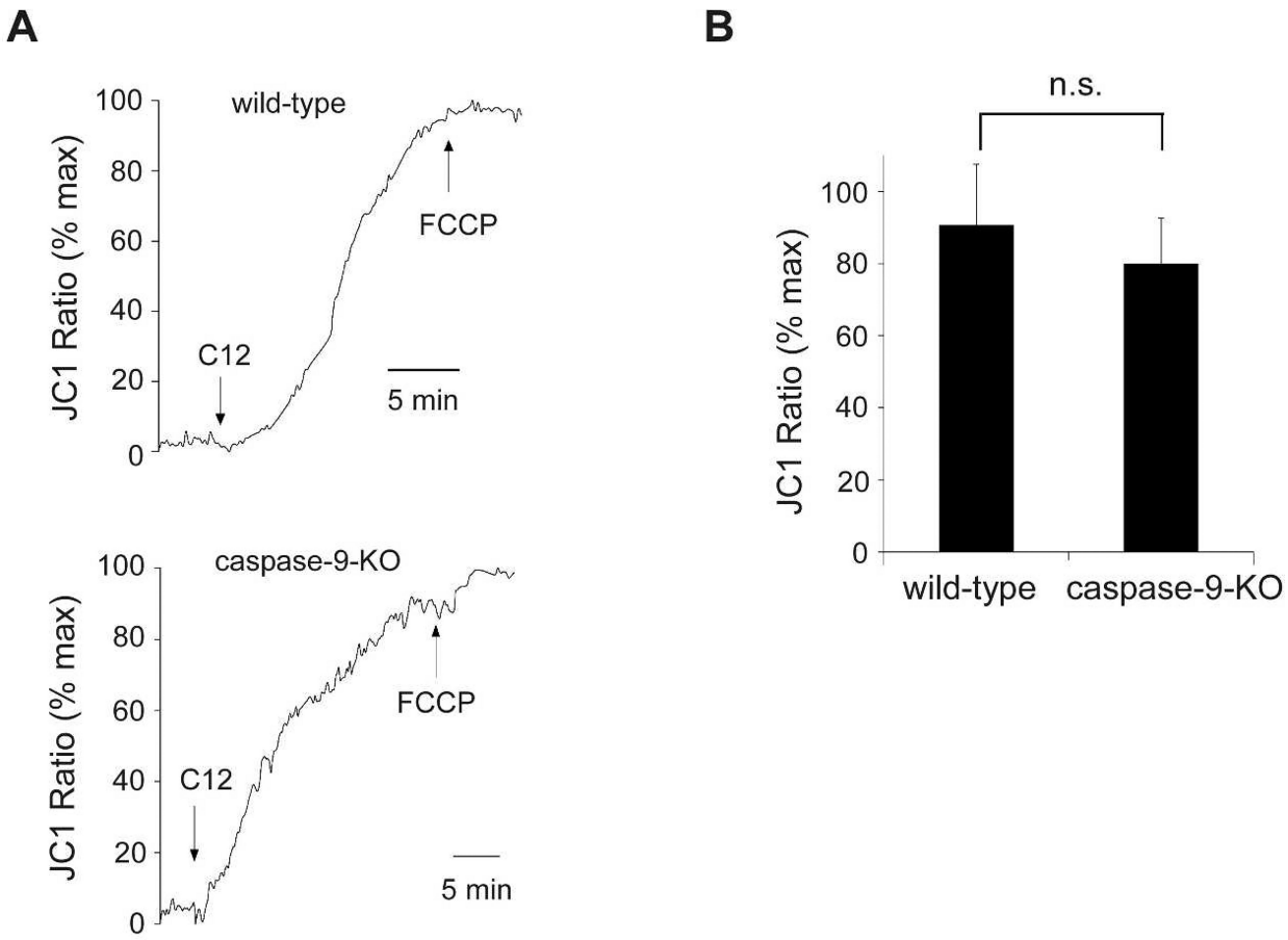

Figure 6. C12-induced mitochondrial potential decrease is independent of caspase-9

(A) Wild-type (WT) and caspase-9-KO MEFs were loaded with JC1, and fluorescence was measured using imaging microscopy during sequential treatment with 50 μM C12 and 10 μM FCCP. Depolarization of $\Delta\psi_{mito}$, equivalent to the increase in JC1 fluorescence, was observed in both WT and caspase-9-KO MEFs following C12 treatment. The data are depicted as the percentage of maximal JC1 fluorescence increase evoked by FCCP. Typical results from three independent experiments are shown. **(B)** Summary of depolarization of $\Delta\psi_{mito}$ in WT and caspase-9-KO MEFs. The level of steady-state depolarization of $\Delta\psi_{mito}$ induced by C12 in WT and caspase-9-KO MEFs was presented as the percentage of the value of maximal depolarization of $\Delta\psi_{mito}$ caused by FCCP. The data are shown as means ± standard deviations of three independent experiments like those in (A). Student's unpaired t test. ns, no significance.

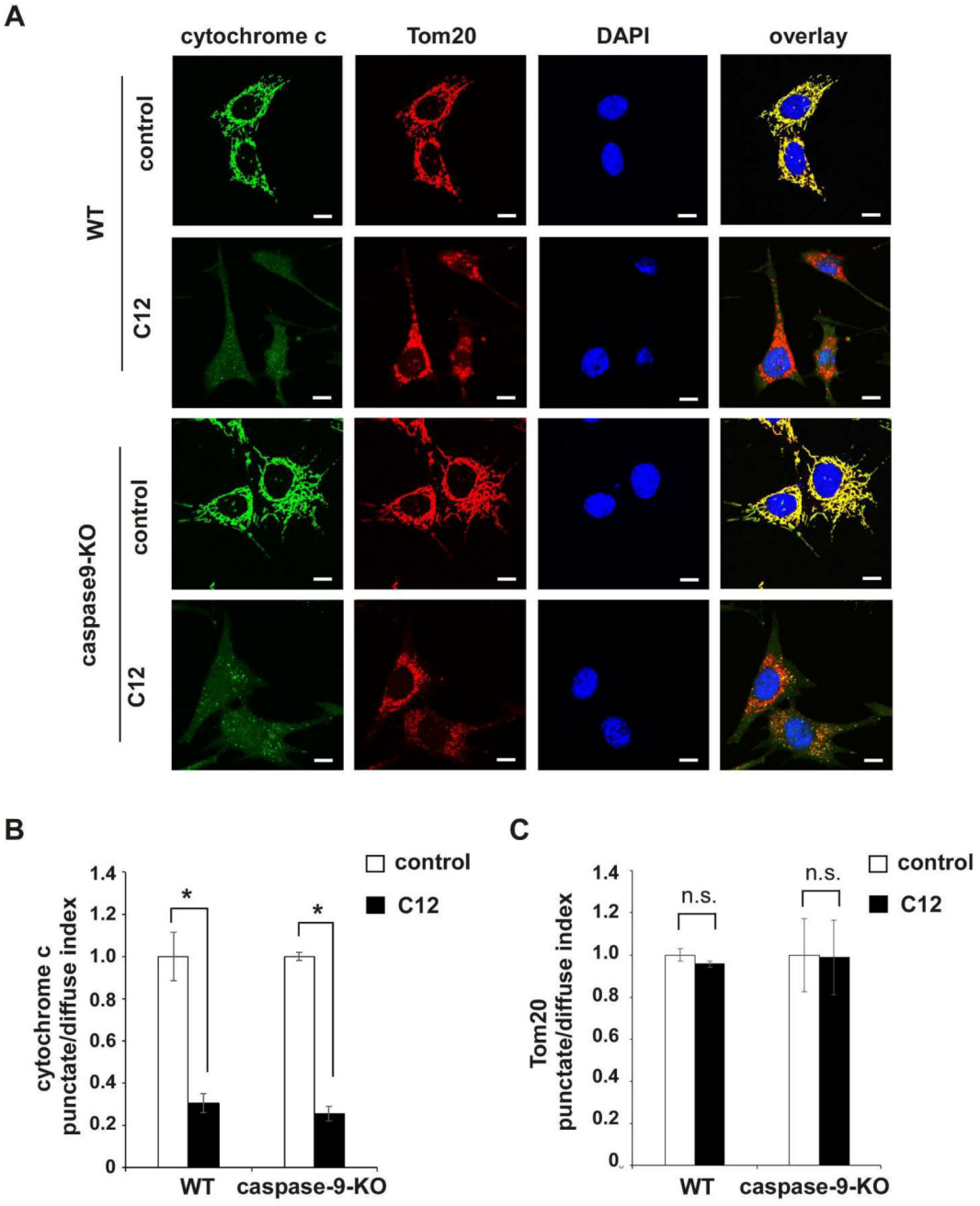

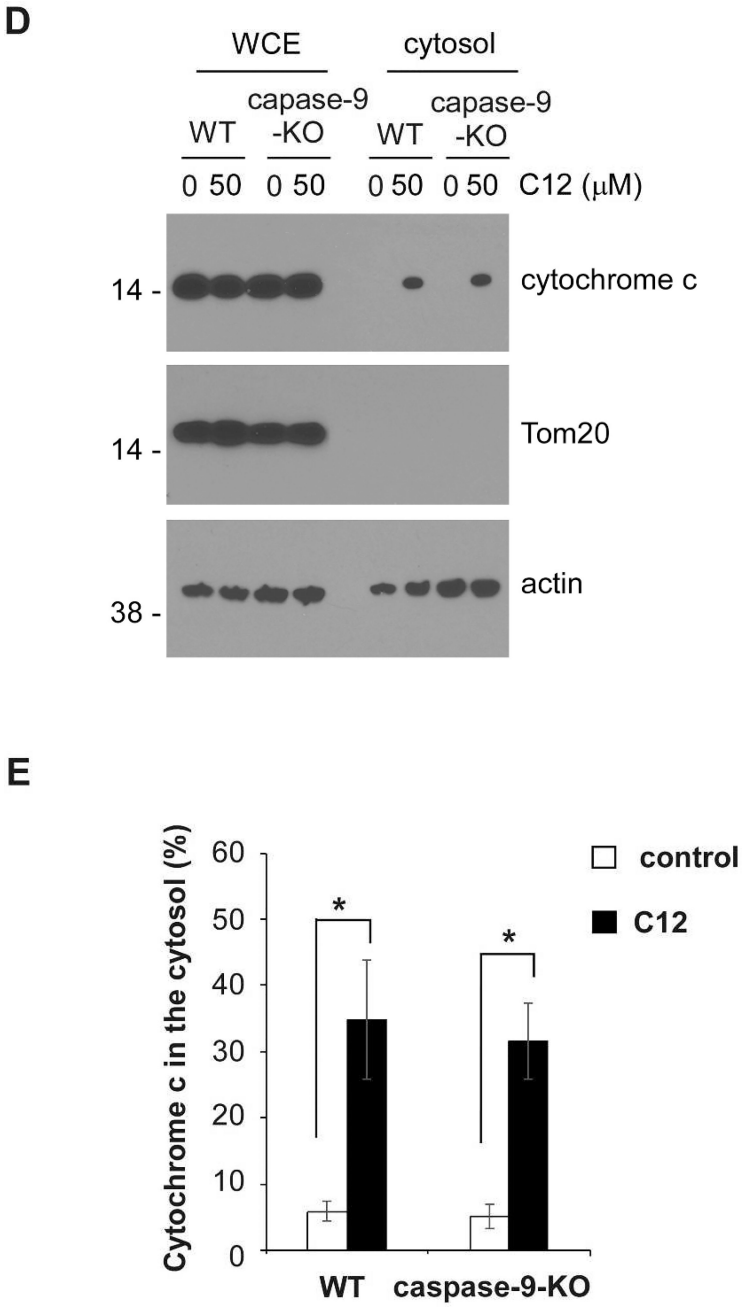

Figure 7. C12-induced caspase-9 activation occurs downstream of mitochondrial membrane permeabilization

(A) Representative confocal images of wild-type (WT) and caspase-9-KO MEFs treated with either DMSO (control) or 50 μM C12 for 4 hours. Tom20 is shown in red, cytochrome c in green, and DAPI in blue. Scale bar, 10 μm. **(B–C)** Summary data showing the intracellular distribution of cytochrome c (B) and Tom20 (C) upon C12 exposure. The punctate/diffuse indexes of intracellular cytochrome c and Tom20 were calculated respectively. The data are the means ± standard deviations of three independent experiments with at least 100 cells calculated in each experiment. Asterisks indicate $P < 0.05$ (*), ns, no

significance. Student's unpaired t test. **(D)** WT and caspase-9-KO MEFs were treated with either DMSO or 50 μM C12 for 4 hours. The cytosolic fractions were acquired. Representative western blot images of isolated fractions were shown (typical of three independent experiments). The molecular weight markers are labeled on the left (kD). **(E)** The amounts of cytochrome c in the whole cell extracts and the cytosolic fractions shown in (D) were quantified using ImageJ software (NIH). As described in Materials and Methods, the normalized values of cytochrome c levels in the cytosolic fractions were calculated as a percentage of relative cytochrome c levels in the corresponding whole cell extracts. Means ± standard deviations of three independent experiments are shown. Asterisks indicate $P < 0.05$ (*); Student's unpaired t test.

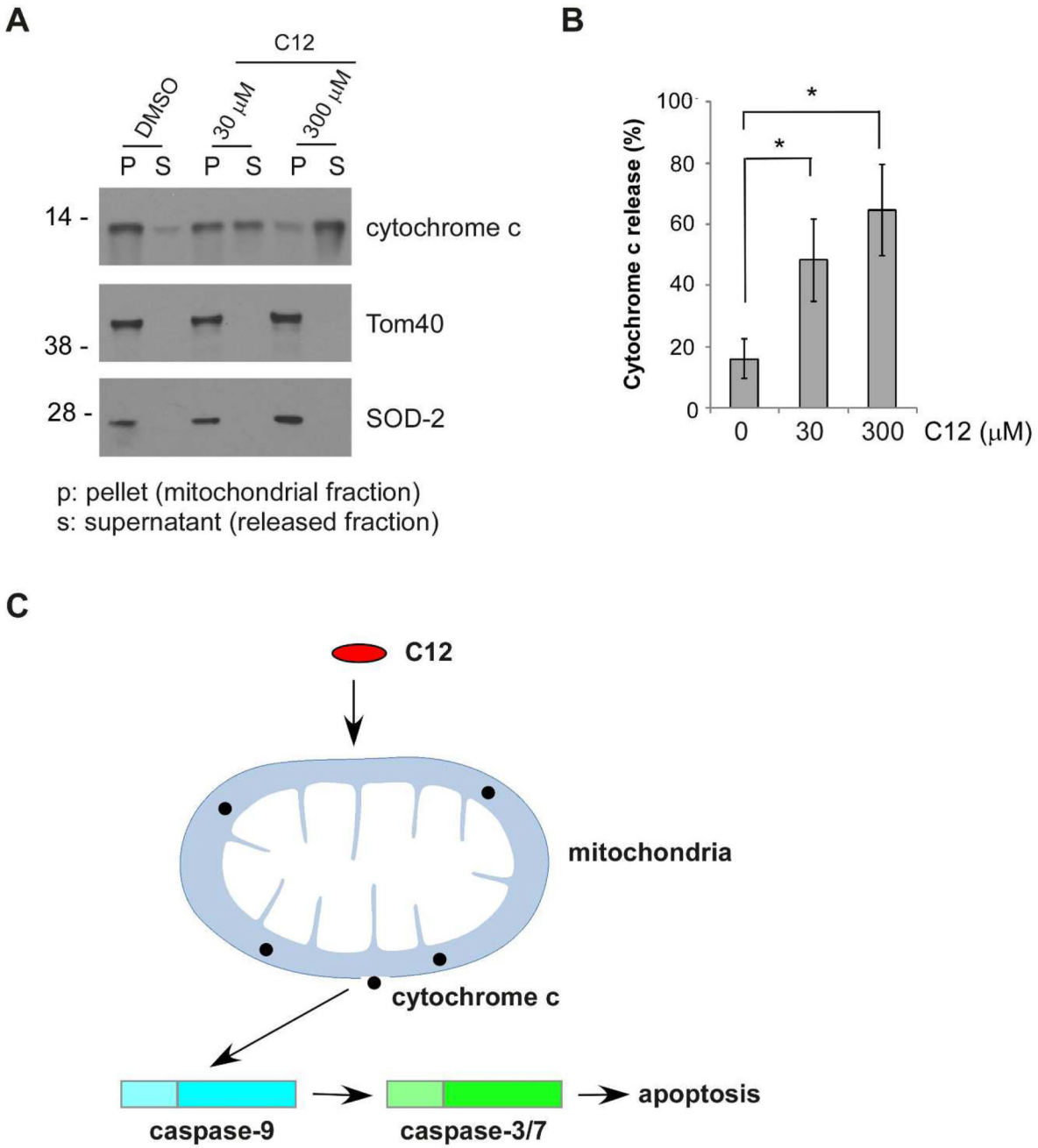

Figure 8. C12 directly induces mitochondrial outer membrane permeabilzation *in vitro*

(A) Mitochondria were isolated from wild-type MEFs and incubated with C12 for 1 hour. Each sample contained 1% DMSO. Release of cytochrome c from mitochondria was determined by western blot. The molecular weight markers are labeled on the left (kD). **(B)** The intensities of cytochrome c in the mitochondrial (P) and the cytosolic (S) fractions shown in (A) were quantified using ImageJ. Cytochrome c release is represented as a percentage of the sum of the protein intensity in mitochondrial and released fractions. Mean ± standard deviation for four independent experiments are shown. Asterisks indicate P <

0.05 (*) by Student's unpaired t test. **(C)** C12 permeabilizes mitochondria, subsequently activating apoptotic signaling pathway.